



Fall 2022

Promoting pinto abalone (*Haliotis kamtschatkana*) recovery in the Salish Sea: The effects of fluctuating temperature and elevated CO₂ on survival, growth, and radula morphology

Elizabeth Janie Diehl

Western Washington University, ejdiehl361@gmail.com

Follow this and additional works at: <https://cedar.wwu.edu/wwuet>



Part of the [Biology Commons](#)

Recommended Citation

Diehl, Elizabeth Janie, "Promoting pinto abalone (*Haliotis kamtschatkana*) recovery in the Salish Sea: The effects of fluctuating temperature and elevated CO₂ on survival, growth, and radula morphology" (2022). *WWU Graduate School Collection*. 1142.
<https://cedar.wwu.edu/wwuet/1142>

This Masters Thesis is brought to you for free and open access by the WWU Graduate and Undergraduate Scholarship at Western CEDAR. It has been accepted for inclusion in WWU Graduate School Collection by an authorized administrator of Western CEDAR. For more information, please contact westerncedar@wwu.edu.

**Promoting pinto abalone (*Haliotis kamtschatkana*) recovery in the Salish Sea: The effects of
fluctuating temperature and elevated CO₂ on survival, growth, and radula morphology**

By

Elizabeth Janie Diehl

Accepted in Partial Completion
of the Requirements for the Degree
Master of Science

ADVISORY COMMITTEE

Dr. Deborah Donovan, Chair

Dr. Brooke Love

Dr. Brady Olson

GRADUATE SCHOOL

David L. Patrick, Dean

Master's Thesis

In presenting this thesis in partial fulfillment of the requirements for a master's degree at Western Washington University, I grant to Western Washington University the non-exclusive royalty-free right to archive, reproduce, distribute, and display the thesis in any and all forms, including electronic format, via any digital library mechanisms maintained by WWU.

I represent and warrant this is my original work, and does not infringe or violate any rights of others. I warrant that I have obtained written permissions from the owner of any third party copyrighted material included in these files.

I acknowledge that I retain ownership rights to the copyright of this work, including but not limited to the right to use all or part of this work in future works, such as articles or books.

Library users are granted permission for individual, research and non-commercial reproduction of this work for educational purposes only. Any further digital posting of this document requires specific permission from the author.

Any copying or publication of this thesis for commercial purposes, or for financial gain, is not allowed without my written permission.

Elizabeth Janie Diehl

November 8th, 2022

**Promoting pinto abalone (*Haliotis kamtschatkana*) recovery in the Salish Sea: The effects of
fluctuating temperature and elevated CO₂ on survival, growth, and radula morphology**

A Thesis
Presented to
The Faculty of
Western Washington University

In Partial Fulfillment
Of the Requirements for the Degree
Master of Science

by
Elizabeth Janie Diehl
November 8th, 2022

ABSTRACT

Overharvesting of pinto abalone (*Haliotis kamtschatkana*) in the Salish Sea between 1959 and 1994 caused severe population declines. This led to the Washington Department of Fish and Wildlife classifying pinto abalone as a “species of concern.” The Puget Sound Restoration Fund (PSRF) is committed to help pinto abalone recover by outplanting juveniles at specific sites around the Salish Sea. Survival of outplanted individuals is different at each site, but it is not clear why. Differences in water chemistry parameters, such as temperature and pH, could explain the differences in survival, either through differences in the mean conditions or through short term exposure to more extreme conditions. Future ocean warming and acidification could make fluctuations in water chemistry parameters more severe.

The goal of my thesis was to simulate in lab the outplanting of abalone post-sets in fluctuating temperature and elevated CO₂ conditions. I utilized an ocean acidification system to create atmospheres that affect seawater pH. I hypothesized that temperature fluctuations and high dissolved CO₂ (low pH) will negatively affect survival, growth, and shell and radula morphology. Fluctuating temperatures yielded lower survival and greater growth, determined by mean shell length, compared to constant temperature. High CO₂ yielded comparable survival and smaller growth than low CO₂. Traditional morphological analysis of the radula found that fluctuating temperatures caused the radula to grow in a more compact manner, with smaller teeth formed closer together. Geometric morphological analysis found that radula tooth orientation was not affected by any of the treatments. This is the first study to find any effects of water chemistry on abalone radula morphology. Overall, the presence of a single stressor was detrimental to pinto abalone post-sets. However, the combination of stressors performed similarly to the absence of stressors. This indicates that fluctuating temperature can mitigate the negative effects of high CO₂, possibly by increasing metabolic rate.

In support of pinto abalone recovery efforts, PSRF can utilize my findings to evaluate water chemistry parameters at their outplant sites. I recommend that pinto abalone be outplanted in areas around the Salish Sea that are characterized by near constant temperatures, around 10°C, and low dissolved CO₂ (high pH around 8.2). Due to yearly, seasonal, and weekly changes in water chemistry conditions, constant conditions do not exist. Outplant sites with the smallest fluctuations in water chemistry parameters should be used. In addition, ocean warming and acidification are expected to occur in concert. My findings indicate pinto abalone post-sets should be able to survive and grow under future climate scenarios, when outplanted into both temperatures that fluctuate on weekly scales, from 10°C up to 14°C, and acidification within 0.2 pH units when these conditions occur together, not separately.

ACKNOWLEDGEMENTS

Thank you to my advisor Dr. Deborah Donovan, who provided outstanding support and encouragement throughout this project. Your willingness to engage and guide my passion has shaped me into the scientist I am today. Thank you to Jaclyn Stapleton for being an excellent lab mate and friend. From field trips to pick up organisms to joint presentations, you have been through everything with me and I could not imagine a better person to do all this with!

Thank you to my committee members for their valuable insight and support. Dr. Brooke Love provided water chemistry resources and helped me think deeper about the big picture of my results. Dr. Brady Olson helped Jaclyn and I set up our experiments and joined my committee when I needed additional support. Dr. Ben Miner provided advice on the initial experimental design.

Thank you to the staff at Shannon Point Marine Center, particularly Gene McKeen, for helping coordinate lab space and light microscope time. Thank you to Mike Kraft and the staff at Scientific Technical Services for teaching me how to use the scanning electron microscope. You all have provided me with the tools to study the things I love.

Thank you to previous members of the Donovan lab. Caitlin O'Brien at Puget Sound Restoration Fund helped provide organisms and their food for the experiment. Lillian Kuehl's previous work with post-set abalone radulae provided the procedures and precedent to study this complex structure. Thank you for answering my long emails and sharing your work!

Support for this project came from several sources including, the Shewmaker Internship from the Washington Department of Fish and Wildlife, the Marine and Coastal Science Program 2021 Fellowship, the Ross and Flora 2021 Fellowship, the Enhancement for Graduate Research 2021 Award, the Pacific Northwest Shell Club 2021 Scholarship, and the North Cascades Audubon Society 2021 Scholarship.

Finally, thank you to my incredible family, Alice Anne, Robert, and Madeline, for supporting and encouraging me. I could not have completed this thesis without you!

TABLE OF CONTENTS

ABSTRACT	iv
ACKNOWLEDGEMENTS	v
LIST OF FIGURES	viii
LIST OF TABLES	x
INTRODUCTION	1
Ocean warming and acidification on molluscs.....	1
Ocean warming and acidification on abalone species.....	4
Ocean warming and acidification on radulae.....	7
Pinto abalone.....	10
METHODS	14
Organisms.....	14
Experimental design.....	15
Water chemistry.....	17
Survival.....	17
Shell length.....	18
Shell morphology.....	18
Radula morphology.....	20
RESULTS	26
Water chemistry.....	26
Survival.....	31
Shell length.....	31
Shell morphology.....	35
Radula morphology.....	35
Traditional analysis.....	35
Geometric analysis.....	42
DISCUSSION	47
Fluctuating temperature.....	47
Elevated CO ₂	49
Interaction between temperature and CO ₂	52

Radula.....	53
Conclusion.....	55
LITERATURE CITED.....	58

LIST OF FIGURES

- Figure 1.** Experimental design. Incubators numbered 1 and 4 were held at the constant temperature of 10°C. Incubators 2 and 3 underwent the temperature fluctuation, between 10°C and 14°C. Each incubator housed four experimental chambers (colored rectangles). Half of the chambers received 400 ppm of CO₂ (low CO₂) and the other half received 1200 ppm CO₂ (high CO₂). Blue chambers indicate the constant temperature low CO₂ treatment. Green indicates the constant temperature high CO₂ treatment. Yellow indicates the fluctuating temperature low CO₂ treatment. Red indicates the fluctuating temperature high CO₂ treatment. This color scheme will be consistent throughout the paper. Each experimental chamber held two six-well plates (small black rectangles).....16
- Figure 2.** Microscopy images of forty day old post-set pinto abalone. (A) “Normal” shell morphology with greatest shell length measurement. The shell length of this individual was 800 μm. (B) “Abnormal” shell morphology. White circle highlights where the shell does not adequately cover abalone body. The shell length of this individual was 434 μm. (C) “Abnormal” shell morphology. White circle highlights where the shell appears rough in texture with several ridges. The shell length of this individual was 568 μm.....19
- Figure 3.** Radula measurements (1-6 and 10) for traditional analysis. R indicates the rachidian tooth. L1 and L2 indicate lateral teeth one and two respectively.....22
- Figure 4.** Landmarks for geometric analysis. (A) Thirteen landmarks describing the middle five teeth, L2-L1-rachidian tooth-L1-L2, for geometric analysis. (B) A wireframe connects the thirteen landmarks to help visualize the orientation of teeth in each row.....24
- Figure 5.** Temperature (°C) which post-set abalone experienced on experimental days 18-36, showing two and a half fluctuations. Temperatures are daily means for both incubators in the constant or fluctuating treatment groups. Error bars are ± standard deviation.....27
- Figure 6:** (A) pH, (B) pCO₂, (C) DIC, and (D) Ω_{aragonite} at different temperatures. Columns are means, colored by treatment as consistent with Figure 1. Error bars are ± standard deviation. Within the fluctuating treatments (yellow and red), pH and Ω_{aragonite} tended to decrease at higher temperatures, where the DIC and pCO₂ were increasing. The high CO₂ treatments (green and red) tended to have lower pH and Ω_{aragonite} and higher DIC and pCO₂ than the low CO₂ treatments (blue and yellow).....29
- Figure 7.** Percent survival of post-set abalone in the four treatment groups over the five week experimental time. The points are mean percent survival and error bars are ± standard deviation.....32
- Figure 8.** Mean shell length (μm) of post-set abalone in the four treatments. Columns represent mean. Error bars are ± standard deviation. Numbers in parentheses indicate sample size (n).....36
- Figure 9.** Percent normal shelled pinto abalone in the four treatments. Columns represent mean. Error bars are ± standard deviation. Numbers in parentheses indicate sample size (n).....37

Figure 10. Rachidian tooth height (μm) as a function of estimated shell length (μm) for the four treatment groups. The red and yellow lines are below the blue and green lines, indicating rachidian tooth height is negatively affected by fluctuating temperature (Table 3).....38

Figure 11. Number of marginal teeth (count) as a function of estimated shell length (μm) for the four treatment groups. Fluctuating temperature increased the number of marginal teeth, illustrated by the yellow line on top. High CO_2 decreased the number of marginal teeth, illustrated by the green line on bottom (Table 3).....39

Figure 12. Cusp Length (μm) as a function of estimated shell length (μm) for the four treatment groups. The red and green lines are generally below the blue and yellow lines, indicating cusp length was negatively affected by high CO_2 (Table 3).....40

Figure 13. Results of a principal components analysis (PCA) for radula shape. Graph is a PCA score plot with points of PCA scores for individual radula. Colors are consistent with Figure 1. On the x-axis, wireframe of principal component one (PC1). Light blue is the radula orientation for a PC1 of 0.0. Dark blue shows a high PC1 score, with the outer dark blue lines on the inside and the rachidian tooth positioned lower than the light blue lines, illustrating a row that is flat. On the y-axis, wireframe of principal component two (PC2). Light blue is the radula orientation for a PC2 of 0.0. Dark blue shows a high PC2 score, with the rachidian tooth to the right.....43

Figure 14. A phylogenetic tree illustrating the relatedness between the four treatment groups for principal component one (PC1) and principal component two (PC2). Similar treatment regimens do not have similar scores, indicating that the treatments did not affect radula orientation.....45

Figure 15. Overlapping wireframes demonstrate the differences in orientation of the middle five radula teeth for each treatment. Light blue is the average orientation for all of the treatments (PC1 and PC2 scores are 0.0). Other colors represent the average orientation of the treatment group as consistent with Figure 1. Constant temperature low CO_2 (dark blue) has a flat vertical orientation with the rachidian tooth to the right. Constant temperature high CO_2 treatment (green) has a vertical orientation near the middle, between flat and arched (PC1 score near 0.0) and the rachidian tooth is far to the left. Fluctuating temperature low CO_2 treatment (yellow) has a more flat vertical orientation and the rachidian tooth is slightly to the left. Fluctuating temperature high CO_2 treatment (red) has an arched vertical orientation with the rachidian tooth to the right.....46

LIST OF TABLES

Table 1. Water chemistry parameters for each treatment group over the forty day experimental time. DIC indicates dissolved inorganic carbon. $\Omega_{\text{aragonite}}$ denotes the saturation state for aragonite. Numbers represent mean \pm standard deviation.....	28
Table 2. Regression outputs from best-fit models for survival, shell length, shell morphology, and all radula morphology traditional analyses. The binomial error structure used with <i>glmer</i> and <i>glm</i> analyses for percent survival and shell morphology respectively generated <i>z</i> values. All other values in this column are <i>t</i> values from <i>lm</i> analysis for shell length and <i>glm</i> analyses for most traditional radula morphology parameters. I analyzed full radula length using an <i>lmer</i> analysis, which does not include p values in its output. In this case, <i>t</i> values > 1.96 are considered significant.....	33
Table 3. Linear equations for trend lines in Figures 10, 11, and 12.....	41
Table 4. Procrustes ANOVA output for geometric radula morphological analysis.....	44

INTRODUCTION

Over the past several decades there has been an increase in anthropogenic atmospheric carbon dioxide (CO₂) (IPCC 2014, Orr et al. 2005). The increase in atmospheric CO₂ has several negative impacts on the ocean and marine life. First, excess CO₂ is trapping more heat in the atmosphere causing ocean temperatures to rise (IPCC 2014). Second, excess CO₂ is dissolving into the ocean where it is changing seawater chemistry, making the ocean more acidic in a process called ocean acidification (OA) (Orr et al. 2005).

The Salish Sea, off the northwest coast of Washington State, has experienced an overall increase in OA, with an average pH decline of 0.22 units over the past 25 years (Lowe et al. 2019). Considerable fluctuations in temperature and pH occur due to changing tides, rain, runoff, and other influences. Seasonal fluctuations of pH in the Salish Sea ranged on average 0.43 units from summer to winter (Lowe et al. 2019). These seasonal fluctuations were strongly correlated with changes in dissolved oxygen, temperature, and salinity. However, pH was not strongly correlated with atmospheric CO₂, indicating that seasonal changes in pH were associated with net changes in respiration (Lowe et al. 2019). Increasing atmospheric CO₂ can alter normal seasonal and weekly fluctuations in pH and make them more extreme, either through causing fluctuations to reach more extreme values or by increasing the duration of extreme events (Cummings et al. 2019, Evans et al. 2019, Lowe et al. 2019).

Ocean warming and acidification on molluscs

Calcifying organisms, such as molluscs, are disproportionately impacted by ocean warming and acidification compared to non-calcifying organisms (Kroeker et al. 2013). This is

due to acidification lowering the saturation of calcium carbonate in seawater which makes the process of shell building more energetically costly (Keppel et al. 2015, Kroeker et al. 2010, Kroeker et al. 2014). Seasonal fluctuations in pH can also affect when calcifying organisms are able to make their shells. Aragonite and calcite are two forms of calcium carbonate important for shell formation. The likelihood of supersaturation of aragonite (aragonite saturation state [$\Omega_{\text{aragonite}}$] > 1) in the Salish Sea is less than 20% in the winter and more than 80% in the summer (Lowe et al. 2019). This means that it is potentially easier for calcifying organisms to build shells in the warmer summer months, when there is a greater amount of aragonite available and seawater pH is more basic.

Ocean warming and acidification have the greatest impact on the early developmental stages of molluscs when the process of calcification is most important, causing a decrease in larval abundance and recruitment (Byrne et al. 2011, Keppel et al. 2015, Li et al. 2013, Petraitis and Dudgeon, 2020). For example, recruitment of blue mussel (*Mytilus edulis*) larvae declined on average 15.7% per year over a fifteen year study time. The average recruitment of 158 individuals per 40 cm² in 2000, fell to an average of 21 individuals per 40 cm² in 2015 (Petraitis and Dudgeon, 2020, Supplementary Data). These findings were correlated with an increase in summer ocean temperatures, from 14.67°C in 2001 to 15.92°C in 2015, an average increase of 0.085°C per year (Petraitis and Dudgeon, 2020, Supplementary Data). During the summer months blue mussels are in their pelagic larval stage, indicating that ocean warming has a significant negative correlation with survivorship of this early life stage.

Increasing the energetic cost of calcification is not the only effect that ocean warming and acidification can have on shells. Shells can also dissolve back into low pH water in a process called dissolution. Shells from four species of South African mussels were exposed to crossed

temperature (14°C and 20°C) and pH (7.5 and 8.0) conditions for 39 days (Emanuel et al. 2020). The amount of shell dissolution was determined by measuring the dry weight of the shells weekly. Three out of four species saw increased shell dissolution (up to 3% shell weight lost) under increased temperature and low pH conditions (Emanuel et al. 2020). This makes molluscs more susceptible to predation under ocean warming and acidification as shell dissolution makes it easier for predators to break open thinner shells (Kroeker et al. 2014).

Other biological processes such as reproduction and foraging are also affected by OA. Severe acidification (pH of 7.1 and 6.7) negatively affected gametogenesis in oysters (*Crassostrea virginica*) such that their reproduction was unsuccessful (Boulais et al. 2017). Under a combination of ocean warming and acidification treatments, the sea hare (*Stylocheilus striatus*) exhibited changes in foraging behaviors such as a reduction in the ability to detect food and a reduction in speed to find food (Horwitz et al. 2020). Additionally, the metabolic rate of the sea hare was elevated by the combination of low pH and high temperature.

These impacts are important to understand not only because of the ecological importance of mollusc species, but the economic importance as well. Mollusc species make up several important fisheries around the world and in the Salish Sea (Barton et al. 2015). For example, upwelling events along the Washington-Oregon coast brought seawater with a pH of 7.6 and low aragonite saturation to the surface in the summers of 2007 and 2008. This caused a mass die-off of oyster larvae at the Whiskey Creek Shellfish Hatchery, leading to a 75% decrease in commercial shellfish larvae production (Barton et al. 2015). This greatly affected the ability of shellfish growers in the Pacific Northwest to pursue their livelihoods. Extensive monitoring of seawater carbonate chemistry at the hatchery in subsequent years provided evidence that natural fluctuations in carbonate chemistry are magnified by OA which can detrimentally affect the

survival and development of commercial shellfish larvae (Barton et al. 2015). Shellfish growers continue to invest in methods to mitigate current and future ocean acidification in their hatcheries, however, wild populations of several important fisheries species cannot be monitored and cared for in this way. This makes the continued investigation of how wild fisheries are responding to ocean warming and acidification paramount.

Ocean warming and acidification on abalone species

Abalone (genus *Haliotis*) are a group of molluscs that are susceptible to ocean warming and acidification due to these conditions impairing their ability to form and maintain shells (Morash and Alter, 2016). To build shells, abalone take up calcium carbonate ions from the environment and then excrete them as aragonite and/or calcite (depending on life history stage and the particular layer of shell) using specialized cells in the ectoderm tissue of the outer mantle (Byrne et al. 2011, Gaume et al. 2011). Abalone have the ability to manipulate their internal metabolic processes to alter the pH at the site of calcification (Cummings et al. 2019). This process becomes increasingly energetically costly as the difference between the internal and external pH widens. Investing more energy in shell formation could negatively affect the efficiency of other metabolic processes (Cummings et al. 2019). A thin organic layer called the periostracum protects the shell from the surrounding seawater, preventing dissolution. Damage to this layer by predation or wave action could cause the shell under it to become exposed and dissolve in corrosive water (Cummings et al. 2019).

Almost all abalone species are experiencing severe declines in their population due to stressors including climate change, habitat destruction, and overharvesting. This has spurred

research into the effects of climate change on abalone. The European abalone (*Haliotis tuberculata*) has been extensively studied in relation to future ocean warming and acidification conditions expected for the end of the 21st century (Auzoux-Bordenave et al. 2020, Avignon et al. 2020, Wessel et al. 2018). Ocean pH is predicted to fall approximately 0.3 units, dropping from 8.0 to 7.7 or lower by 2100 (IPCC 2014). European abalone larvae exposed to predicted pH values had lower survival, smaller size, delayed development, shell abnormalities, and decreased shell mineralization (Wessel et al. 2018). European abalone juveniles also exhibited reduced shell length, weight, and strength when exposed to a pH of 7.6 and $\Omega_{\text{aragonite}} < 1$ for three months (Auzoux-Bordenave et al. 2020). The reduced shell length observed was a result of slower growth of new shell area under the low pH treatment and loss of existing shell as it was corroded and dissolved away (Auzoux-Bordenave et al. 2020). European abalone adults exposed to a pH of 7.7 for four months experienced reduced shell strength and calcification due to partial dissolution of outer shell layers (Avignon et al. 2020). This comprehensive picture of the European abalone indicates that all life stages of this species are negatively affected by OA.

Similar to the European abalone, reddish-rayed abalone (*Haliotis coccoradiata*) larva exposed to increased warming (22°C and 24°C) and acidification (pH of 7.8 and 7.6) until 21 hours post-fertilization exhibited lower percentage of calcified individuals due to low $\Omega_{\text{aragonite}}$ (Byrne et al. 2011). Mean percentage of calcified larvae was 60% at normal temperature (20°C) and pH (8.2) but fell to less than 20% at the elevated temperatures and low pH conditions (Byrne et al. 2011). Additionally, red abalone (*Haliotis rufescens*) larva exposed to high temperature and low pH had lower survivorship (Zippay and Hofmann, 2010). In the late veliger stage, survivorship was > 95% at normal temperature (15.5°C) and pH (8.05), but significantly fell to < 90% at 23.6°C and a pH of 7.87 (Zippay and Hofmann, 2010).

Other species of abalone have exhibited resilience to ocean warming and acidification. Green abalone (*Haliotis fulgens*) juveniles were able to recover from short term (hours-days) high temperature (18°C), and pH (6.6) stressors, such that respiration rate matched those individuals unexposed to the stressors (Calderón-Liévanos et al. 2019). Similarly, juvenile New Zealand pāua (*Haliotis iris*) kept for four months in crossed temperature and pH treatments (temperatures of 13°C and 15°C, pH of 8.00 and 7.66) exhibited phenotypic plasticity, adapting to their change in conditions (Cummings et al. 2019). Individuals in this experiment kept at 13°C and a pH of 7.66 experienced an $\Omega_{\text{aragonite}} < 1$, leading to older surface shell layers dissolving away (Cummings et al. 2019). However, new internal shell layers grew thicker, demonstrating a plastic response to dissolution, such that overall shell thickness was not significantly different between treatment groups (Cummings et al. 2019). These results indicate that different species of abalone react to ocean warming and acidification in different ways.

These differences in responses could be due to different adaptations. Upwelling events along the west coast of North America have regularly exposed specific populations of red abalone (*H. rufescens*) to low pH (Swezey et al. 2020). Over time, consistent exposure may have led to resiliency. In a study exposing red abalone from embryo to three months post-settlement to OA conditions, those individuals from populations in locations that experienced regular upwelling had a higher amount of lipid reserve to feed off of during the pelagic larval stage (Swezey et al. 2020). In addition, they had a slower reduction of their lipid reserve, leading to greater survival (Swezey et al. 2020). Those individuals from populations that were not exposed to regular upwelling had a smaller lipid reserve and faster metabolism, leading to decreased survival (Swezey et al. 2020). Thus, consistent exposure to water chemistry differences that are

characteristic of specific locations can have a big impact on how those populations react to ocean warming and acidification.

Ocean warming and acidification on radulae

The radula is a feeding apparatus that allows many species of molluscs, including abalone, to scrape their food off of rocks. Radulae are made out of chitin that is mineralized with calcium, iron, and/or phosphorous (Marchant et al. 2010, Sigwart and Carey, 2014). Radula morphology is an important factor for abalone survival, development, and recruitment because it impacts the ability to consume and digest food, especially in early life stages such as the post-set stage (Kawamura et al. 2001, Kuehl and Donovan, 2020, Onitsuka et al. 2004). As abalone age and grow their diet shifts from benthic diatoms to macroalgae (Neuman et al. 2018). The shape of the radula changes to help facilitate the change in diet. For example, the angle of radula teeth changes as they grow to aid in rupturing diatom frustules during consumption which improves digestion (Kawamura et al. 2001). Similarly, as radula tooth number and size increases, diatom species of larger size and increasing adhesion strength become easier to ingest (Kuehl and Donovan, 2020). The prevalence of serrations on the radula teeth also decreases as abalone age, indicating a transition in feeding from diatoms to macroalgae (Kawamura et al. 2001, Onitsuka et al. 2004). The action of the radula, scraping diatoms or macroalgae off of surfaces, clears the area for other organisms to colonize. Thus, radula morphology is not only important for abalone feeding, it is also important to the ability of abalone to fulfil their ecological niche as a grazer.

The biomineralization processes that form radulae could be affected by ocean warming and acidification in three ways. First, increased temperature tends to increase organism activity

levels and thus the need to consume food. This could increase damage to and wear on radula teeth, potentially wearing teeth down faster than they can be replaced (Marchant et al. 2010, Sigwart and Carey, 2014). Second, increased activity levels also require more energy to go towards respiration which could decrease the amount of energy that can go towards growth (Donovan and Carefoot, 1998). Radula growth specifically is energetically expensive (Marchant et al. 2010). Third, ocean acidification could affect the biomineralization of new radula teeth by removing building blocks from the water, resulting in growth of weaker teeth that could break more easily (Sigwart and Carey, 2014). Direct dissolution of the radula is unlikely because they are not a purely calcium carbonate structure (Marchant et al. 2010). Several studies have examined the impacts of feeding and food type on abalone radula morphology (Kawamura et al. 2001, Kuehl and Donovan, 2020, Onitsuka et al. 2004), however, research into the effects of ocean warming and acidification on the abalone radula is greatly lacking.

Radulae from a few other species of molluscs have been examined in relation to ocean warming and acidification. The chiton *Leptochiton asellus* has a radula that is mineralized with iron magnetite (Sigwart and Carey, 2014). Individuals were added to fully crossed temperature (10°C, 15°C, and 20°C) and CO₂ (400 ppm and 2000 ppm) conditions for four weeks (Sigwart and Carey, 2014). No difference in the mineralization of teeth, total number of rows, or instance of cracks or holes in the radula were found between treatment groups (Sigwart and Carey, 2014). This is a surprising finding considering that the elevated CO₂ conditions had a pH of 7.5 and were undersaturated in aragonite, compared to the control conditions with a pH of 8.0 and supersaturation of aragonite (Sigwart and Carey, 2014). These findings provide evidence that ocean warming and acidification conditions did not disrupt the radula biomineralization pathway, or these stressors were somehow compensated for, perhaps by increased radula growth (Sigwart

and Carey, 2014). Chitons are thus expected to be able to persist under ocean warming and acidification conditions (Sigwart and Cary, 2014).

In contrast to those findings, common limpets (*Patella vulgata*) exposed to short-term (5 days) low pH (7.6) had more broken radula teeth and more wear on teeth measured by area than limpets exposed to normal pH (8.2) (Marchant et al. 2010). Limpet radulae are not mineralized with iron magnetite like chitons, but with calcium and phosphate in hydroxyapatite (Marchant et al. 2010). The exact mechanism behind the observed increase in wear is unknown due to the ability of limpets to maintain internal acid-base balance, metabolism, and feeding rate under the low pH conditions (Marchant et al. 2010). The long term effects of such damage to the radula could result in reduced feeding efficiency and thus reduced survival (Marchant et al. 2010), indicating that limpets may have a difficult time persisting under ocean warming and acidification.

The above studies demonstrate that radulae from different mollusc species are responding differently to ocean warming and acidification. Abalone radulae are likely to be more similar to limpet radulae than to chiton radulae. All three of these species are molluscs, but chitons belong to class Polyplacophora, while limpets and abalone are both in class Gastropoda, indicating that limpets and abalone have more in common with one another. If abalone radula development, growth, or function is compromised by ocean warming and acidification in a similar way to limpets, the ability to eat and graze could be affected, diminishing the ability of abalone to survive and perform their ecosystem functions. This makes understanding the effects of ocean warming and acidification on abalone radula morphology paramount.

Pinto abalone

The pinto abalone (*Haliotis kamtschatkana*) is the only abalone species native to the Salish Sea. Pinto abalone are ecologically important because they are ecosystem engineers, clearing algae from hard surfaces to make way for other organisms to live there. This species has a “low to moderate” risk of extinction due to decreased abundance and has been designated as a “species of concern” by the Washington Department of Fish and Wildlife (WDFW) (Carson and Ulrich, 2019, Neuman et al. 2018). The main cause of historic declines in abundance is overharvesting. The WDFW closed all recreational pinto abalone harvesting in 1994, however, pinto abalone populations have continued to decrease (Carson and Ulrich, 2019).

Surveys of population abundance have been conducted for pinto abalone in the Salish Sea in response to the observed decline. Rogers-Bennett et al. (2011) counted only seventeen total adult pinto abalone, and no juveniles, at ten dive survey sites in 2005, compared to a similar survey in 1979 that found 242 individuals, including juveniles, at fewer sites in less time. Rothaus et al. (2008) found continuous declines in pinto abalone abundance over a time span of fourteen years, from 0.18 individual abalone per square meter in 1992 to 0.04 individual abalone per square meter in 2006, a decline of 77%. Young emergent abalone (shell length of less than 90 mm) comprised 16% of all individuals observed in the early years of their study (1992, 1994, and 1996). In the later years (2003 to 2006), the number of observed young emergent abalone had fallen to less than 6% of observed individuals (Rothaus et al. 2008). There was also an increase in mean shell length over the course of this survey, further indicating that young abalone were absent from the population (Rothaus et al. 2008).

These findings support recruitment failure, where no young individuals are growing up to replace older individuals, in wild pinto abalone populations (Bouma et al. 2012, Petraitis and

Dudgeon, 2020, Rogers-Bennett et al. 2011, Rothaus et al. 2008). This places the pinto abalone in a precarious position because abalone are density dependent for reproduction and require a certain number of individuals in an area (hypothesized density of 0.15 abalone per square meter) for broadcast spawning reproduction to be successful (Babcock and Keesing 1999, Rothaus et al. 2008). Even with long term closure of the recreational fishery, population collapse is still possible due to low population density. Without intervention, the pinto abalone population is unlikely to recover on its own (Rothaus et al. 2008).

The Puget Sound Restoration Fund (PSRF) has answered this need by creating an aquaculture rearing and hatchery facility. Here, pinto abalone are spawned and raised for outplanting, the process of releasing young individuals out into the wild. Outplant efforts have been successful with a one year average survival of 10.2% (Carson et al. 2019). Outplant sites have similar habitat parameters with rocky outcroppings for abalone to hide in and access to the different types of food that abalone eat throughout their life cycle. Temperatures at depth at these outplant sites typically average 9.9-11.0°C during the summer (Carson et al. 2019). Additionally, hatchery individuals have not been observed emigrating from the outplant sites into which they were released, promoting aggregation densities that support successful natural spawning (Carson et al. 2019). However, survival varies greatly between the outplant sites. This variation cannot be explained by lineage or size at outplanting, indicating that survival must be site specific (Carson et al. 2019). Each of the outplanting sites likely vary in their water chemistry conditions, such as temperature range and pH.

Currently, PSRF is outplanting juveniles that are one to two years old, which is successful but also costly. The process of spawning, rearing, and outplanting is costly because of the large amount of resources and time put into each individual. Outplanting abalone as larvae or

post-sets (the intermediate life stage between larva and juvenile beginning after metamorphosis and lasting approximately three months until the first gill opening in the shell is formed and there is a shift in diet from diatoms to macroalgae) could reduce cost and increase success. Mills-Orcutt et al. (2020) investigated this when they experimented with outplanting larvae given a settlement cue into tented and open larval abalone modules in the field. Tented larval abalone modules have 125 μ m Nitex mesh screen around them to help retain the larvae in the immediate area. They found that using tented modules increased larval settlement over open modules and is a plausible avenue for future, lower cost, outplanting methods (Mills-Orcutt et al. 2020). However, this outplanting method will only be effective if the tented larval abalone modules are deployed in areas where the water chemistry conditions, such as temperature and pH, will also promote survival and proper development.

Few studies have directly investigated the impacts of ocean warming and acidification on pinto abalone. Crim et al. (2011) exposed pinto abalone larvae to lower pH conditions created by bubbling specific amounts of CO₂ through treatment tanks. In the lower pH conditions (800 and 1800 ppm of CO₂) only 40% of the larvae survived, compared to 65% survival in the control treatment (400 ppm). Shell deformities increased under lower pH, higher CO₂ levels. Under control conditions, 98% of larvae developed normal shells, while only 60% and 1% of larvae developed normal shells under the 800 ppm and 1800 ppm treatments respectively. Larval shell size was reduced by 5% for the 800 ppm treatment, and could not be determined for the 1800 ppm treatment as there were not enough larvae with shells for the calculation. Surprisingly, the percent settlement, the proportion of larvae that successfully go through metamorphosis, was not impacted by the CO₂ treatments (Crim et al. 2011).

Very little research has been conducted on the pinto abalone radula. Kuehl and Donovan (2020) examined the pinto abalone radula in relation to diet by conducting feeding trials with six different species of diatoms for 61 days post-settlement. They found that *Amphora salina*, yielded the highest survival and *Cylindrotheca closterium* yielded the highest growth (Kuehl and Donovan, 2020). There was no relationship between diet and radula morphology, indicating that pinto abalone do not display morphological plasticity in their radula when presented with different food types. However, overall radula development was similar to other abalone species (Kuehl and Donovan, 2020). No current studies have examined how the pinto abalone radula could be affected by varying ocean warming and acidification conditions.

For my thesis project, I investigated the effects of fluctuating temperature and elevated CO₂ levels on the survival, growth, and shell and radula morphology of post-set pinto abalone. My research helps support the recovery of pinto abalone in the Salish Sea in three ways: (1) by providing a possible explanation for the difference in survivorship noted between the current outplant sites, (2) determining temperature and CO₂ conditions that larval abalone given a settlement cue can be outplanted into, and (3) by examining an understudied life stage and body structure. The results of my study will aid PSRF in the evaluation and selection of outplant sites by recommending temperature and CO₂ conditions which promote pinto abalone survival and proper development. My overarching research question was; how does temperature variation and elevated CO₂ affect the survival, growth, and shell and radula morphology of post-set pinto abalone? My hypothesis was; pinto abalone post-sets reared under fluctuating temperatures (10-14°C) and elevated CO₂ (1200 ppm) will be negatively affected such that there will be lower survival, less growth (lower mean shell length), higher percentage of abnormal shell morphologies, and differences in radula morphology.

METHODS

Organisms

I obtained approximately 4,000 *Haliotis kamtschatkana* larvae at seven days post-fertilization from the Kenneth K. Chew Center for Shellfish Research and Restoration at NOAA's Research Station run by the Puget Sound Restoration Fund in Manchester, Washington. The larvae were produced in a mixed family of one female crossed with three males so the larvae were either full or half siblings. I transported the larvae in an aerated four liter plastic jar in a cooler to the Shannon Point Marine Center in Anacortes, Washington. Larvae were in transit for four hours and upon arrival were acclimated to 10°C for 20 hours (12:12 light cycle).

To inoculate the larval abalone into the experimental wells, I poured the larvae over a 100 µm Nitex mesh screen. Then, I pipetted thirteen individuals into each well of thirty-two six-well plates and added filtered seawater (FSW) to a final volume of 10 mL. FSW used in this experiment was filtered to 2 µm. I added gamma aminobutyric acid (GABA) to each well at a final concentration of 4 µM to induce the larvae to metamorphose into the post-set stage and settle at the bottom of the wells. After approximately an hour and a half of exposure to GABA, I conducted two 80% water changes in succession to remove GABA.

I fed the post-larvae a combination diet of three species of diatoms; *Amphora salina*, *Cylindrotheca closterium*, and *Navicula salinicola* which promotes survival and growth and is the diet used by PSRF at their hatchery (Kuehl and Donovan, 2020). I added the diatom food to each well of each six well plate by pipetting in approximately 2 mL of concentrated diatom solution once a week during week one and week two of my experiment. After this time, the diatom films were established and growing on their own, so no additional diatoms were added.

Experimental Design

Two temperature regimens (constant and fluctuating) were crossed fully with two levels of CO₂ (400 ppm and 1200 ppm). The constant temperature regimen was 10°C. The fluctuating temperature regimen changed from 10°C to 14°C and back to 10°C with one degree increments of change per day so a full cycle took eight days. To create the temperature regimens, I utilized four incubators total: three free-standing incubators and one walk-in incubator. I assigned two incubators to each temperature regimen: one free-standing incubator and the walk-in incubator at constant temperature (Incubators 1 and 4) and two free-standing incubators for fluctuating temperature (Incubators 2 and 3) (Figure 1). The fluctuating temperature regimen required reprogramming the temperature on the appropriate free-standing incubators daily.

The CO₂ levels were created using the system described by Love et al. (2017). Ambient air from the laboratory room was drawn into a CO₂ scrubber. Precise amounts of research grade CO₂ gas (99% CO₂, AirGas) were then combined with the CO₂ stripped air to create both the 400 ppm CO₂ (low CO₂) and 1200 ppm CO₂ (high CO₂) treatments. Treated air was bubbled through a small beaker in each environmental chamber to reduce evaporation and salinity changes in the six-well plates. Treated air was also bubbled into carboys for use during weekly water changes. Four hundred ppm of CO₂ produced a higher pH of approximately 8.24. Twelve hundred ppm of CO₂ produced a lower pH of approximately 8.00.

Two six-well plates were randomly placed into each of sixteen experimental chambers. Four chambers were placed into each incubator where half the chambers received 400 ppm CO₂ and half received 1200 ppm CO₂ (Figure 1). Unless otherwise specified, the experimental unit was the six-well plate and there were eight plates per treatment.

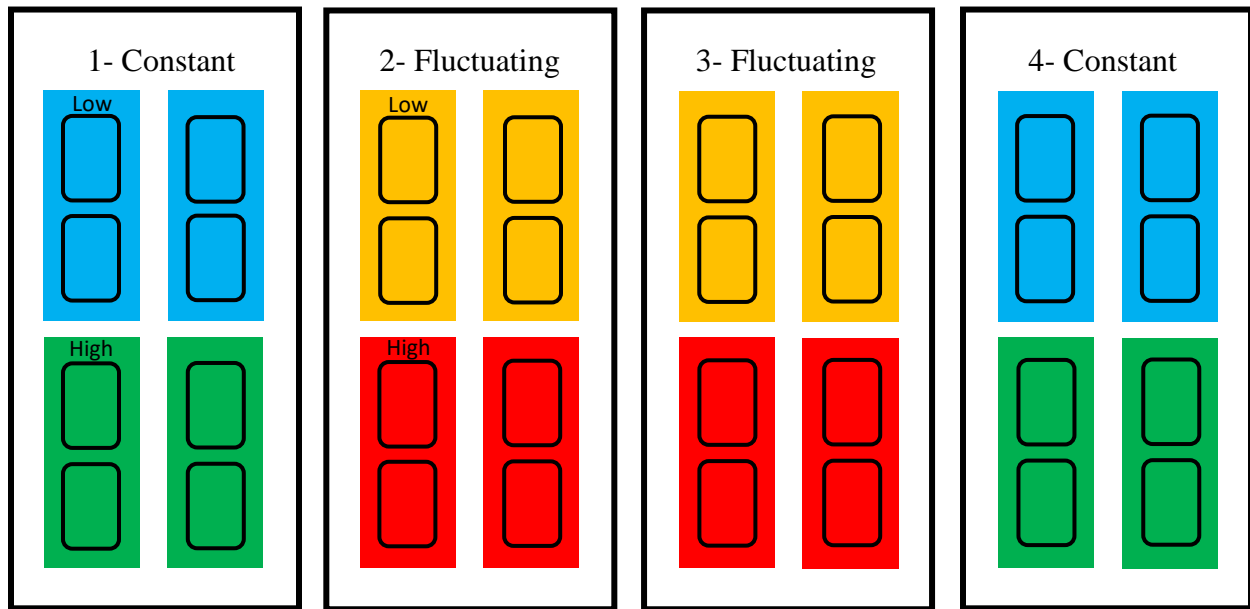


Figure 1. Experimental design. Incubators numbered 1 and 4 were held at the constant temperature of 10°C. Incubators 2 and 3 underwent the temperature fluctuation, between 10°C and 14°C. Each incubator housed four experimental chambers (colored rectangles). Half of the chambers received 400 ppm of CO₂ (low CO₂) and the other half received 1200 ppm CO₂ (high CO₂). Blue chambers indicate the constant temperature low CO₂ treatment. Green indicates the constant temperature high CO₂ treatment. Yellow indicates the fluctuating temperature low CO₂ treatment. Red indicates the fluctuating temperature high CO₂ treatment. This color scheme will be consistent throughout the paper. Each experimental chamber held two six-well plates (small black rectangles).

Water Chemistry

Once a week after collecting survival data (below), I conducted a water change. Five mL of water were removed from each well and replaced with enough FSW, pre-treated at 10°C with the appropriate CO₂ treatment, to fill the wells back up to 10 mL. Water removed from each well was combined for each six-well plate to ensure the water sample would be large enough for later pH, dissolved inorganic carbon (DIC), and salinity analysis. I transferred 20 mL of the combined water to a scintillation vial and fixed it with 10 µL mercuric chloride. Samples were stored at 2°C before analysis which occurred within three weeks from collection. I measured pH using an Ocean Optics S-UV-VIS flame spectrophotometer. Water samples were warmed in a 25°C water bath before being transferred to a 5 cm jacketed cuvette. Samples then received two additions of 20 µL m-cresol dye to determine absorbance at 730 nm, 578 nm, and 434 nm wavelengths. I measured DIC with an Apollo SciTech AS-C3 DIC Analyzer. I measured salinity using a refractometer. I input measured pH, DIC, and salinity values into CO₂SYS (Pelletier et al. 2012) to calculate pH (total scale), pCO₂, and aragonite saturation state ($\Omega_{\text{aragonite}}$). These methods are consistent with Lawlor and Arellano (2020).

I collected temperature data using iButtons (iButtonLink) set to record temperature every 15 minutes at 0.5°C accuracy. I placed one iButton in a small glass dish in each incubator on the same level as the experimental chambers.

Survival

Once a week for five weeks I removed each six-well plate from its environmental chamber and viewed it under a dissecting light microscope (Leica Microsystems, Buffalo Grove,

IL). I counted every living post-set abalone in each well and compared the new count with the initial count to determine the percent survival. I analyzed percent survival using a general linear mixed model with binomial error function.

Shell length

At the end of the five-week experimental time, I gently dislodged all living post-set abalone from the sides of the well and positioned them on their foot at the bottom of each well. I photographed the post-set abalone alongside a 1 cm scale bar using a stereoscope equipped with a camera (Leica Microsystems, Buffalo Grove, IL). I used ImageJ (Rasband, 1997) to measure the greatest shell length (μm) of each individual (Figure 2A). Then, I took the mean shell length (μm) per six-well plate. During a four day period between the final survival data collection and the shell length photographing, a high mortality event occurred in Incubator 4, resulting in 0% survival in this incubator. Thus, Incubator 4 was excluded from this data collection. I analyzed shell length using a general linear mixed model. I captured images over three days, but day was not a significant predictor of shell length.

Shell morphology

I acquired photos of each individual at the same time as the scale bar photos used for the above shell length (μm) data collection. I visually assessed the shell morphology of each individual as being “normal,” “abnormal,” or “unknown,” using the procedures outlined by Crim et al. (2011). “Normal” shell morphology was defined as the shell appearing smooth, round, and

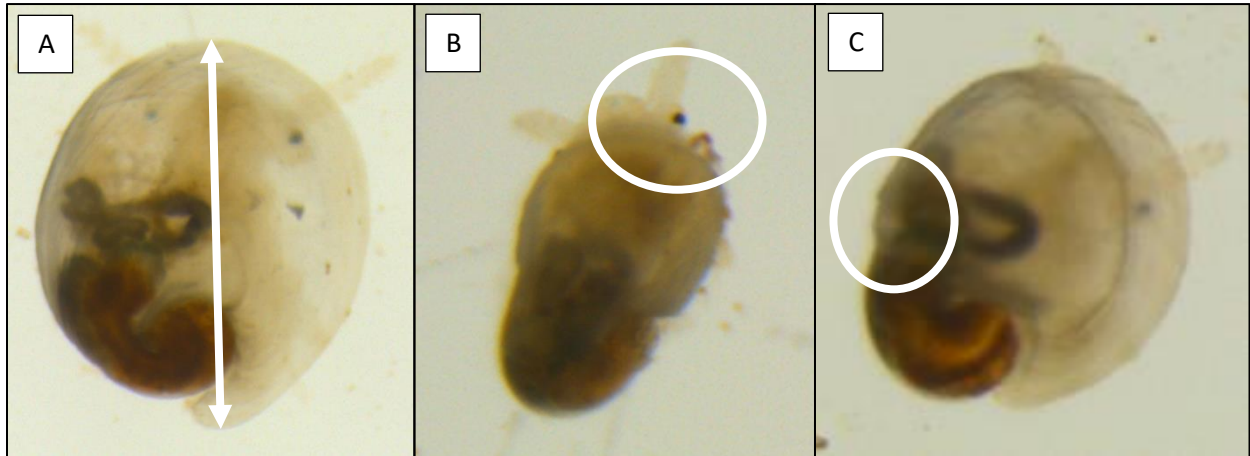


Figure 2. Microscopy images of forty day old post-set pinto abalone. (A) “Normal” shell morphology with greatest shell length measurement. The shell length of this individual was 800 μm . (B) “Abnormal” shell morphology. White circle highlights where the shell does not adequately cover abalone body. The shell length of this individual was 434 μm . (C) “Abnormal” shell morphology. White circle highlights where the shell appears rough in texture with several ridges. The shell length of this individual was 568 μm .

covering a majority of the abalone body (Figure 2A). “Abnormal” shells did not adequately cover the abalone body or appeared rough in texture (Figure 2 B and C). I analyzed the proportion of normal individuals for each six-well plate for each treatment using a general linear mixed model with binomial error function.

Radula morphology

After the above photos were collected, I preserved all remaining living post-set abalone in deionized water and froze them in a -4°C freezer. To extract each radula for imaging, I thawed each post-set abalone and added it to a 6% sodium hypochlorite (bleach) solution to dissolve soft tissues. I then moved the radula through a series of washes in deionized water to remove any remaining tissue. When thoroughly rinsed, I placed each radula on a thin plastic sheet to dry. I then transferred each radula to an aluminum scanning electron microscope stub using double-stick carbon tape. The stubs were coated in gold sputter before I placed them into a scanning electron microscope (Vega TS 5136 MM, TESCAN, Kohoutovice, Czech Republic) to obtain images. These methods are consistent with Kuehl and Donovan (2020).

I conducted two different types of morphometric analyses: traditional and geometric. For the traditional analysis, I took ten descriptive measurements for each radula: (1) rachidian tooth cusp length (fold to tip), (2) rachidian tooth height (base to fold), (3) rachidian tooth base width (across the widest part of the base), (4) gap length (distance between rows measured from rachidian tooth base to rachidian tooth base), (5) number of lateral teeth per row, (6) number of marginal teeth per row, (7) total number of rows in full length of the radula, (8) buccal cartilage position (row number at which the posterior ends of buccal cartilages terminate), (9) full length

of the radula (distance from the top of the radula to the base of the last formed row), and (10) full width of the radula (Figure 3). For all of the above measurements (except for 7, 8, and 9), I measured multiple rows and averaged them to create a single datum for each measurement per radula (Kuehl and Donovan, 2020). I collected measurements from 110 total radulae (the constant temperature low CO₂ treatment had 26 individuals, the constant temperature high CO₂ treatment had 17 individuals, the fluctuating temperature low CO₂ treatment had 35 individuals, and the fluctuating temperature high CO₂ treatment had 32 individuals) using ImageJ (Rasband, 1997).

The statistical analysis of the traditional measurements included shell length as a predictor to help eliminate and explain any variation which overall size of the individual, not the treatments, could cause. I collected shell length data as described above but could not confidently connect shell lengths to radula measurements for each individual. In order to recreate that connection, I used the regression equations created by Kuehl and Donovan (2020). I selected their equations for radula length, radula width, rachidian tooth height, and gap length due to their high R² values. I averaged the predicted shell lengths determined by these equations together and compared them with the actual shell lengths I had previously collected. I assigned an actual shell length to each radula, choosing the value which most closely matched the prediction. I conducted this process for each plate so that the pool from which I was selecting shell length measurements corresponded closely to the pool of radula measurements. For example, I collected from plate labeled “AF,” eight actual shell length measurements and seven sets of radula measurements. I used the average estimated shell lengths determined by the regression equations to help reconnect each set of radula measurements to an actual shell length. I am confident that this process successfully matched shell lengths and radula measurements correctly such that shell

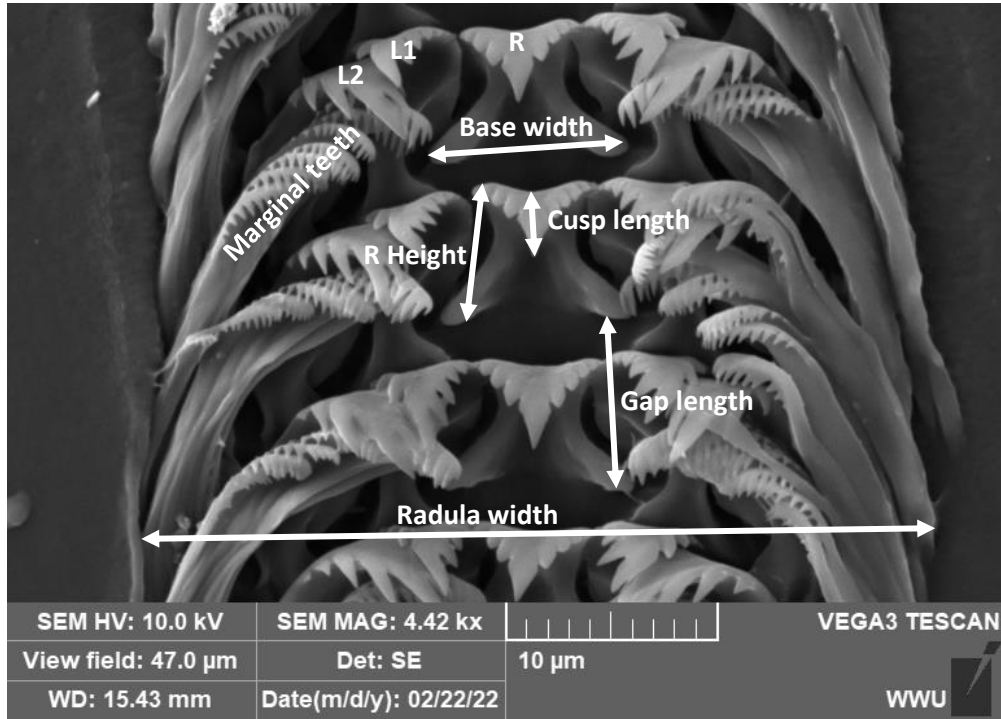


Figure 3. Radula measurements (1-6 and 10) for traditional analysis. R indicates the rachidian tooth. L1 and L2 indicate lateral teeth one and two respectively.

length can be used as a fixed factor in the regression analysis to help explain variation due to the overall size of the individual, not the treatments. If I were to do this experiment again, I would preserve individuals separately and collect shell length data on the same day as dissections.

I used simple linear regressions to determine if the treatments had any effect on each of the traditional descriptive measurements. I used a model selection procedure recommended by Zuur et al. (2009). This procedure began with the most complex model that included only fixed factors. Then, random factors were added and tested for parsimony using AIC values. Lastly, fixed factors were removed from the models to determine the most parsimonious model that contains both fixed and random effects. I treated each radula as an individual due to the limited number of successful dissections and the small amount of variation which the random variables (incubator, box, and plate) explained. All of the radulae had the same number of lateral teeth so I did not conduct a regression analysis for this descriptive measurement.

I based the geometric analysis on a set of thirteen two-dimensional landmarks which describe the relative positions of the middle five teeth in each row of the radula (Figure 4). The first step in this analysis was an extensive elimination process to ensure that the radulae could be properly compared. I based the first elimination on shell length, removing the smallest ten and largest thirty individuals. The overall size of the individual could potentially influence the geometric analysis by artificially causing landmarks to be further apart. This elimination has the same overall effect as adding shell length did to the traditional regression. I based the second round of eliminations on the flexibility of the radula, examining the SEM images to see if they were in a flat and straight orientation in the image or if they were bent, mangled, or upside down. Bending of the radula would artificially cause some landmarks to be further away than others, obscuring the possible effects of the treatments. I based the third elimination on imaged row

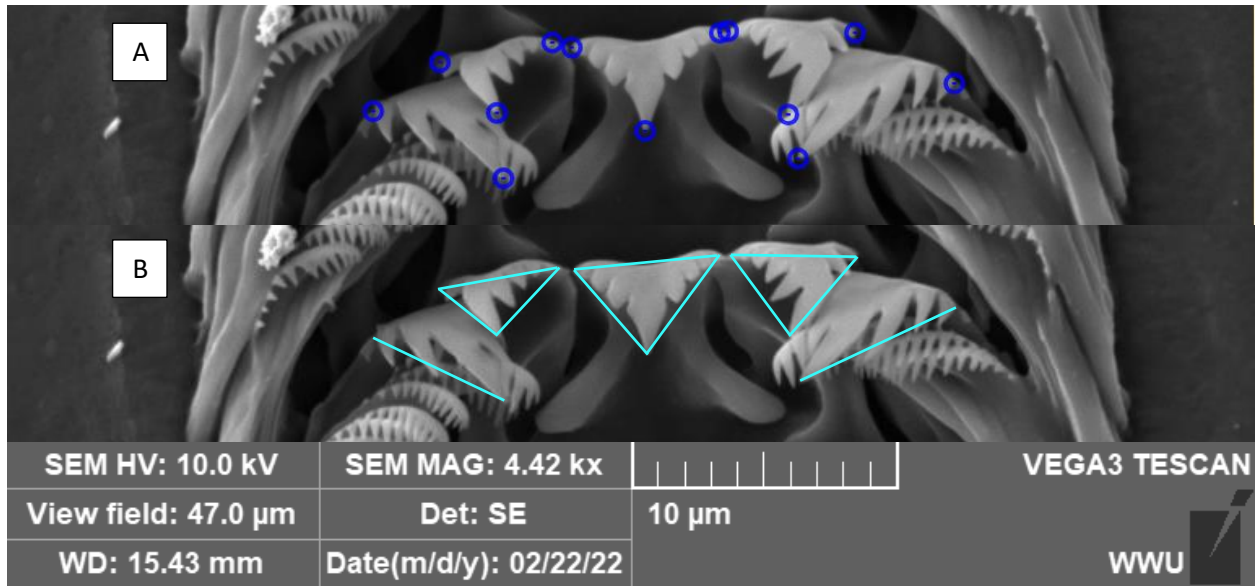


Figure 4. Landmarks for geometric analysis. (A) Thirteen landmarks describing the middle five teeth, L2-L1-rachidian tooth-L1-L2, for geometric analysis. (B) A wireframe connects the thirteen landmarks to help visualize the orientation of teeth in each row.

numbers. The overall width of the radula generally changes from being broader at the top to skinnier at the bottom. Placing landmarks on the same set of rows for each radula avoids any effect that row number, and not the treatments, would have on the geometric analysis. I chose to landmark row numbers three through eight. I landmarked a total of 73 rows from 28 radulae (the constant temperature low CO₂ treatment had 18 rows from 8 radulae, the constant temperature high CO₂ treatment had 11 rows from 4 radulae, the fluctuating temperature low CO₂ treatment had 18 rows from 7 radulae, and the fluctuating temperature high CO₂ treatment had 26 rows from 9 radulae). Landmarks were created using the program StereoMorph (Olsen and Westneat, 2015).

After I completed landmarking, I conducted a Generalized Procrustes Analysis on each row to align the landmarks. Then, I averaged the aligned landmarks for each row per radula so there were one set of landmarks for each radula. Bilateral symmetry was not assumed for the radulae. I then conducted a Procrustes ANOVA using the Geomorph package (Adams and Otarola-Castillo, 2013) in R on the averaged landmarks to compare the orientation of the middle five radula teeth between treatments. I also conducted a principal components analysis (PCA) and created the descriptive figures in the results section using MorphoJ (Klingenberg, 2011).

RESULTS

Water Chemistry

Water chemistry varied over this experiment in expected and unexpected ways. The temperature treatments generally followed the planned treatment regimens (constant at 10°C and fluctuating between 10-14°C, Figure 5). There were differences in temperature, occasionally up to 2°C, between day and night caused by the lighting cycle heating the incubators during the day. The maximum temperature recorded was 14.96°C. The minimum temperature recorded was 9.51°C. The temperature fluctuation affected pH through an increase of energy in the system: more H⁺ ions dissociate at higher temperatures, corresponding with a lower pH (Table 1, Figure 6A).

An unexpected variation in water chemistry was the amount of pCO₂ measured. The planned CO₂ treatments were 400 ppm CO₂ for the low CO₂ treatment and 1200 ppm CO₂ for the high CO₂ treatment. I monitored the CO₂ gas concentrations bubbled into the beakers in the environmental chambers and the carboys using a LI-820 CO₂ Gas Analyzer embedded in the ocean acidification system (Love et al. 2017). The pCO₂ leaving the ocean acidification system consistently met desired levels. However, the photosynthetic diatom food and water changes affected the amount of pCO₂ post-set abalone were exposed to during this experiment (this will be expanded on later in the Discussion section). These sources of modification led to the measured pCO₂ values being much lower than predicted, around 289 ppm for the low CO₂ treatment and 608 ppm for the high CO₂ treatment (Table 1). However, pH still appears to be affected as a result of the CO₂ treatment with the high CO₂ treatment groups having a corresponding lower pH (Table 1, Figure 6).

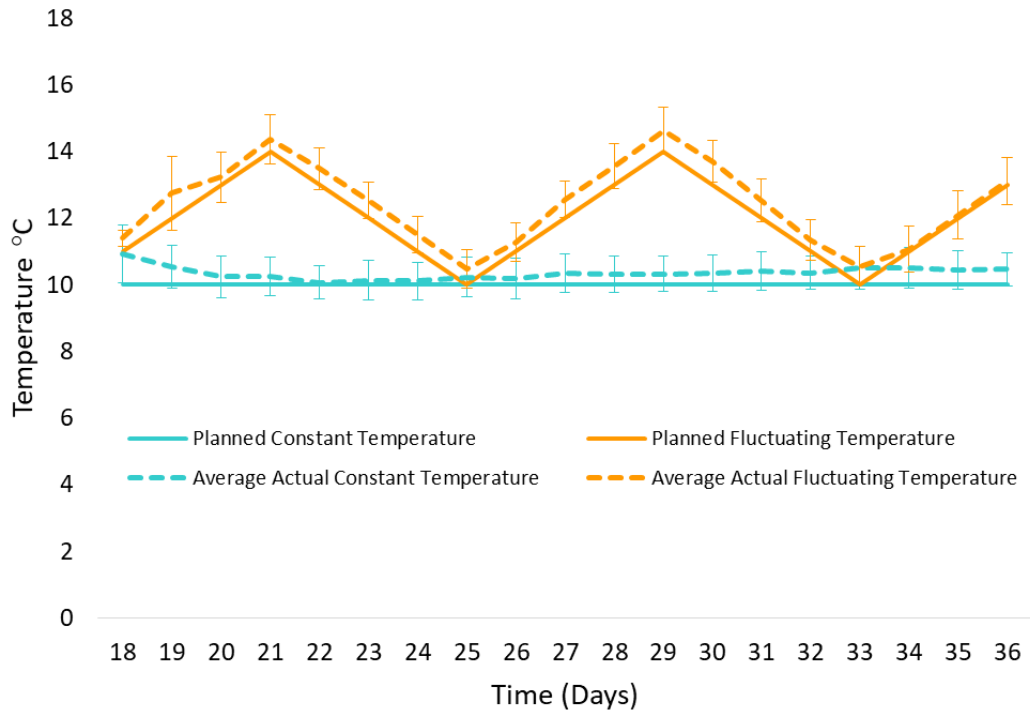


Figure 5. Temperature (°C) which post-set abalone experienced on experimental days 18-36, showing two and a half fluctuations. Temperatures are daily means for both incubators in the constant or fluctuating treatment groups. Error bars are \pm standard deviation.

Table 1. Water chemistry parameters for each treatment group over the forty day experimental time. DIC indicates dissolved inorganic carbon. $\Omega_{\text{aragonite}}$ denotes the saturation state for aragonite. Numbers represent mean \pm standard deviation.

Treatment name:	pH:	pCO ₂ (μatm):	DIC ($\mu\text{mol/kg}$):	$\Omega_{\text{aragonite}}$:	Salinity (ppt):
Constant temperature low CO ₂	8.32 \pm 0.20	238.37 \pm 127.34	2078.59 \pm 344.56	3.43 \pm 1.06	32.38 \pm 1.19
Constant temperature high CO ₂	8.03 \pm 0.25	556.93 \pm 348.72	2321.13 \pm 417.89	2.24 \pm 1.26	32.13 \pm 2.10
Fluctuating temperature low CO ₂	8.16 \pm 0.14	332.94 \pm 131.16	2123.44 \pm 232.97	2.81 \pm 0.64	32.60 \pm 2.12
Fluctuating temperature high CO ₂	7.97 \pm 0.22	646.69 \pm 388.92	2339.26 \pm 355.79	2.14 \pm 0.91	33.20 \pm 2.94

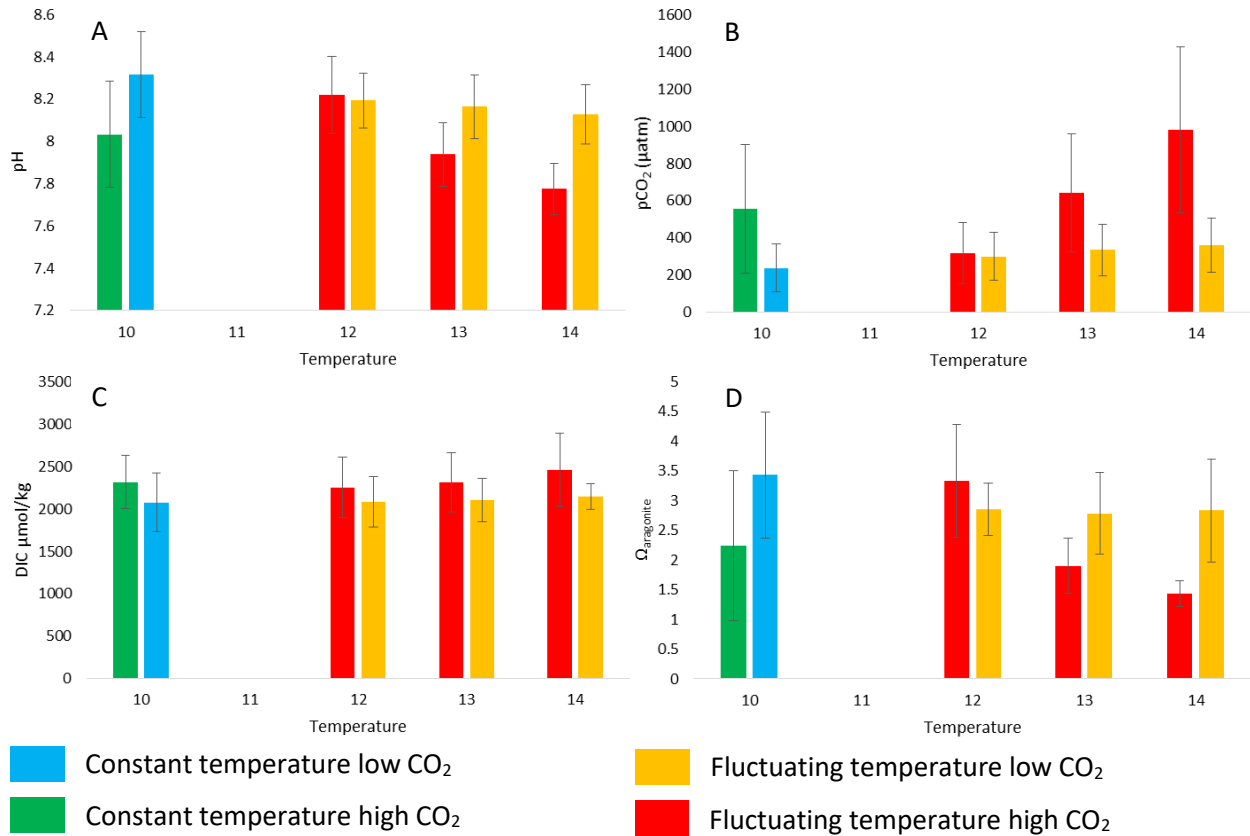


Figure 6: (A) pH, (B) pCO₂, (C) DIC, and (D) Ω_{aragonite} at different temperatures. Columns are means, colored by treatment as consistent with Figure 1. Error bars are ± standard deviation. Within the fluctuating treatments (yellow and red), pH and Ω_{aragonite} tended to decrease at higher temperatures, where the DIC and pCO₂ were increasing. The high CO₂ treatments (green and red) tended to have lower pH and Ω_{aragonite} and higher DIC and pCO₂ than the low CO₂ treatments (blue and yellow).

Another unexpected variation in water chemistry was a general increase in salinity throughout the experiment. Treated air added to experimental chambers was bubbled through a beaker of water to attempt to prevent evaporation, and thus an increase in salinity, from occurring in the wells. However, water used during weekly water changes was pre-treated with CO₂ by constantly bubbling the CO₂ treatments into two different carboys. This likely caused evaporation to occur and salinity to increase in the carboy water reserves. The replacement water used during weekly water changes that should have helped control the salinity contributed to the unexpected increase. Salinity in this experiment did not exceed abalone tolerance range of 25-45 ppt and also mostly stayed in the optimal range of 30-35 ppt (Morash and Alter, 2016). The minimum salinity measured in this experiment was 30 ppt and the maximum salinity measured was 39 ppt. All of the treatment groups experienced similar changes in salinity over the course of the experiment (Table 1), so any effects of salinity should be felt by all the treatment groups.

Aragonite was supersaturated over the course of the experiment with $\Omega_{\text{aragonite}} > 1$ in all treatment groups (Table 1). $\Omega_{\text{aragonite}}$ was affected by pH with lower $\Omega_{\text{aragonite}}$ corresponding to lower pH measurements (Table 1). $\Omega_{\text{aragonite}}$ should also be affected by temperature such that higher temperatures increase $\Omega_{\text{aragonite}}$ by increasing precipitation (Kroeker et al. 2013), however, higher temperatures corresponded to lower $\Omega_{\text{aragonite}}$ within the fluctuating temperature treatments (Figure 6D). The effect of pH on $\Omega_{\text{aragonite}}$ thus appears stronger than that of temperature within the ranges of this study.

Solubility of gases decreases at higher temperatures, so the concentration of CO₂ in the six-well plates at the “top,” (14°C) of the fluctuating temperature regimen was expected to be less than at the “bottom,” (10°C). However, this was not directly observed in my experiment due to higher amounts of DIC corresponding to higher temperatures within the fluctuating

temperature treatment groups (Figure 6C), though there was little overall difference. This could indicate that there is a lag between the temperature change and the change in CO₂ concentration due to the process of diffusion happening slowly.

Survival

The fluctuating temperature treatment groups (yellow and red lines) had higher survival, (> 85%) than the constant temperature treatment groups (blue and green lines, < 85%) during the first three weeks of the experiment (Figure 7). During week four, however, the average percent survival of the fluctuating temperature treatment groups dropped to < 70%, becoming similar to the constant temperature treatment groups. Both the constant temperature treatment groups (blue and green lines) and the fluctuating temperature high CO₂ treatment group (red line) ended the experiment with ~33% survival (Figure 7). The fluctuating temperature low CO₂ treatment (yellow line) had significantly lower, 12%, survival (Figure 7). Survival of post-set abalones at week five was best predicted by the interaction of temperature regimen and CO₂ treatment as fixed factors, and box as a random factor (Table 2). Under constant temperature conditions, CO₂ had little effect. However, under fluctuating temperature conditions, CO₂ did affect survival with the low CO₂ treatment having lower average percent survival at week five (Figure 7, $p < 0.001$).

Shell Length

Shell length of post-sets was best predicted by temperature regimen and CO₂ treatment as fixed factors with no interaction (Table 2, $R^2 = 0.70$). AIC was not improved by adding incubator

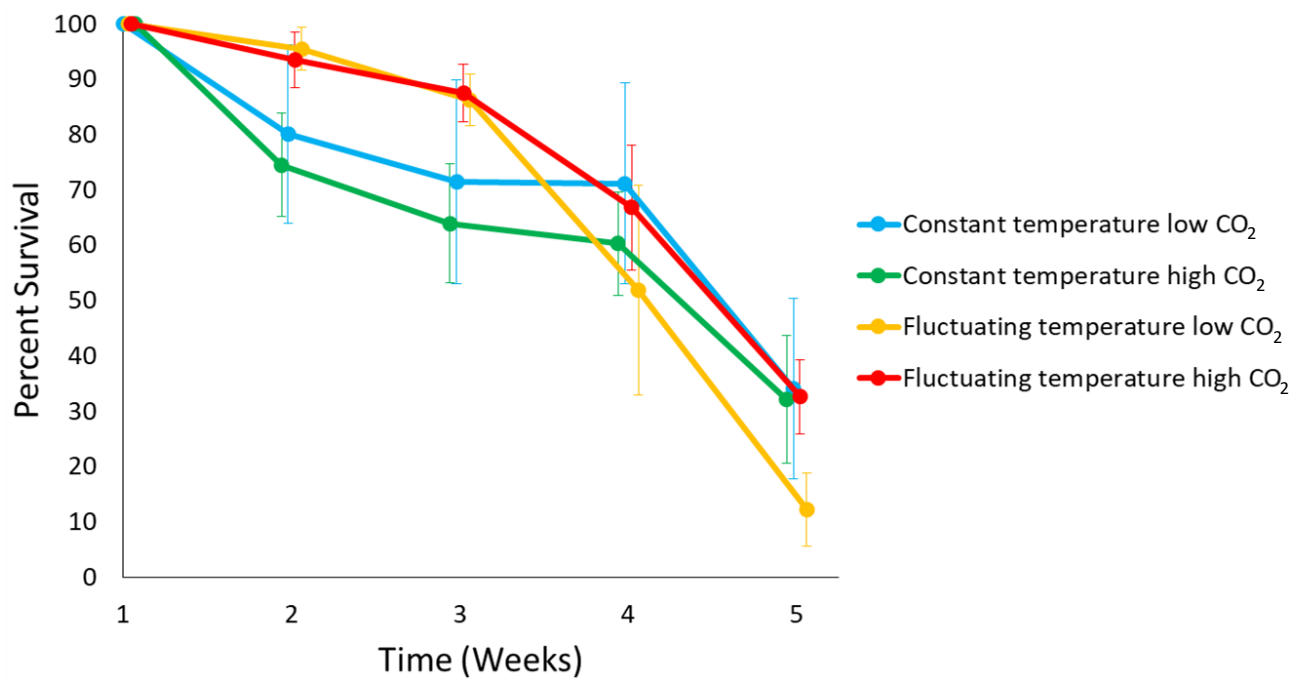


Figure 7. Percent survival of post-set abalone in the four treatment groups over the five week experimental time. The points are mean percent survival and error bars are \pm standard deviation.

Table 2. Regression outputs from best-fit models for survival, shell length, shell morphology, and all radula morphology traditional analyses. The binomial error structure used with *glmer* and *glm* analyses for percent survival and shell morphology respectively generated *z* values. All other values in this column are *t* values from *lm* analysis for shell length and *glm* analyses for most traditional radula morphology parameters. I analyzed full radula length using an *lmer* analysis, which does not include *p* values in its output. In this case, *t* values > 1.96 are considered significant.

		Estimate ± SE	<i>t</i> or <i>z</i> value	<i>p</i> value
Percent Survival	<i>End, Start ~ Temperature * CO₂ + (Box)</i>			
	Intercept	-1.10 ± 0.12	-9.12	< 0.001
	Temperature (ref: Constant)	-1.01 ± 0.19	-5.25	< 0.001
	CO ₂ (ref: low)	-0.05 ± 0.17	-0.32	0.75
	Interaction	1.04 ± 0.26	4.03	< 0.001
Shell Length	<i>Mean Shell Length ~ Temperature + CO₂</i>			
	Intercept	560.70 ± 18.62	30.12	< 0.001
	Temperature (ref: Constant)	136.25 ± 19.75	6.90	< 0.001
	CO ₂ (ref: low)	-56.72 ± 18.62	-3.05	0.006
Shell Morphology	<i>Normal, Total ~ Temperature + CO₂</i>			
	Intercept	-0.61 ± 0.21	-2.90	0.00377
	Temperature (ref: Constant)	0.28 ± 0.23	1.21	0.23
	CO ₂ (ref: low)	-0.038 ± 0.22	-0.17	0.87
Traditional Radula Morphological Analysis				
Cusp Length	<i>Cusp Length ~ CO₂ + Shell Length</i>			
	Intercept	0.721 ± 0.293	2.456	0.015
	CO ₂ (ref: low)	-0.207 ± 0.083	-2.494	0.014
	Shell Length	0.004 ± < 0.001	9.988	< 0.001
Rachidian Tooth Height	<i>Rachidian Tooth Height ~ Temperature + Shell Length</i>			
	Intercept	2.586 ± 0.307	8.415	< 0.001
	Temperature (ref: Constant)	-0.419 ± 0.101	-4.145	< 0.001
	Shell Length	0.007 ± 0.001	12.658	< 0.001
Rachidian Tooth Base Width	<i>Base Width ~ Shell Length</i>			
	Intercept	3.206 ± 0.415	7.728	< 0.001
	Shell Length	0.010 ± 0.001	15.210	< 0.001
Gap Length	<i>Gap Length ~ Temperature + Shell Length</i>			
	Intercept	0.552 ± 0.356	1.550	0.124
	Temperature (ref: Constant)	-0.711 ± 0.117	-6.069	< 0.001
	Shell Length	0.012 ± 0.001	19.504	< 0.001

Number of Marginal Teeth	<i>Marginal Teeth ~ Temperature + CO₂ + Shell Length</i>			
	Intercept	1.965 ± 1.333	1.474	0.144
	Temperature (ref: Constant)	1.533 ± 0.414	3.700	< 0.001
	CO ₂ (ref: low)	-1.727 ± 0.353	-4.892	< 0.001
	Shell Length	0.016 ± 0.002	7.413	< 0.001
Total Rows	<i>Total Rows ~ Temperature + Shell Length</i>			
	Intercept	7.051 ± 1.963	3.592	< 0.001
	Temperature (ref: Constant)	1.487 ± 0.686	2.169	0.033
	Shell Length	0.018 ± 0.003	5.375	< 0.001
Buccal Cartilage Position	<i>Buccal Cartilage ~ Shell Length</i>			
	Intercept	6.197 ± 1.396	4.439	< 0.001
	Shell Length	0.008 ± 0.002	3.665	< 0.001
Full Length	<i>Full Length ~ Temperature + CO₂ + Shell Length + (Box)</i>			
	Intercept	-40.791 ± 20.167	-2.023	
	Temperature (ref: Constant)	2.809 ± 8.796	0.319	
	CO ₂ (ref: low)	-8.715 ± 8.029	-1.086	
	Shell Length	0.310 ± 0.031	9.971	
Full Width	<i>Full Width ~ Temperature + Shell Length</i>			
	Intercept	1.306 ± 1.773	0.737	0.463
	Temperature (ref: Constant)	-1.375 ± 0.602	-2.286	0.024
	Shell Length	0.051 ± 0.003	16.912	< 0.001

and/or box as random factors. The fluctuating temperature treatment groups (yellow and red columns) yielded a greater mean shell length by 136 μm (26%) compared to the constant temperature treatment groups (blue and green columns) ($t = 6.90$, $p < 0.001$, Figure 8). The low CO_2 treatment groups (blue and yellow columns) yielded greater mean shell length by 56 μm (9%) than the high CO_2 treatment groups (green and red columns) ($t = 3.05$, $p = 0.006$, Figure 8).

Shell Morphology

High CO_2 appeared to lower the proportion of normal shelled individuals, exhibited by the constant temperature high CO_2 group (green column) having a lower average percent normal (49%) than the other treatment groups (~71%) (Figure 9). However, shell morphology of post-set abalone was not significantly affected by either temperature regimen or CO_2 treatment (Table 2).

Radula Morphology

Traditional Analysis

Shell length significantly impacted all the descriptive radula measurements as predicted: larger radula measurements belonged to larger abalone (Table 2). Different descriptive measurements were affected in different ways by the treatments. Overall, temperature fluctuation caused more teeth to be formed closer together. Specifically, fluctuating temperature decreased rachidian tooth height (Figure 10), gap length, and full width of the radula (Table 2). Fluctuating temperature also increased the total number of rows and the number of marginal teeth (Figure 11). Overall, the high CO_2 treatment yielded smaller teeth with decreased cusp length (Figure 12)

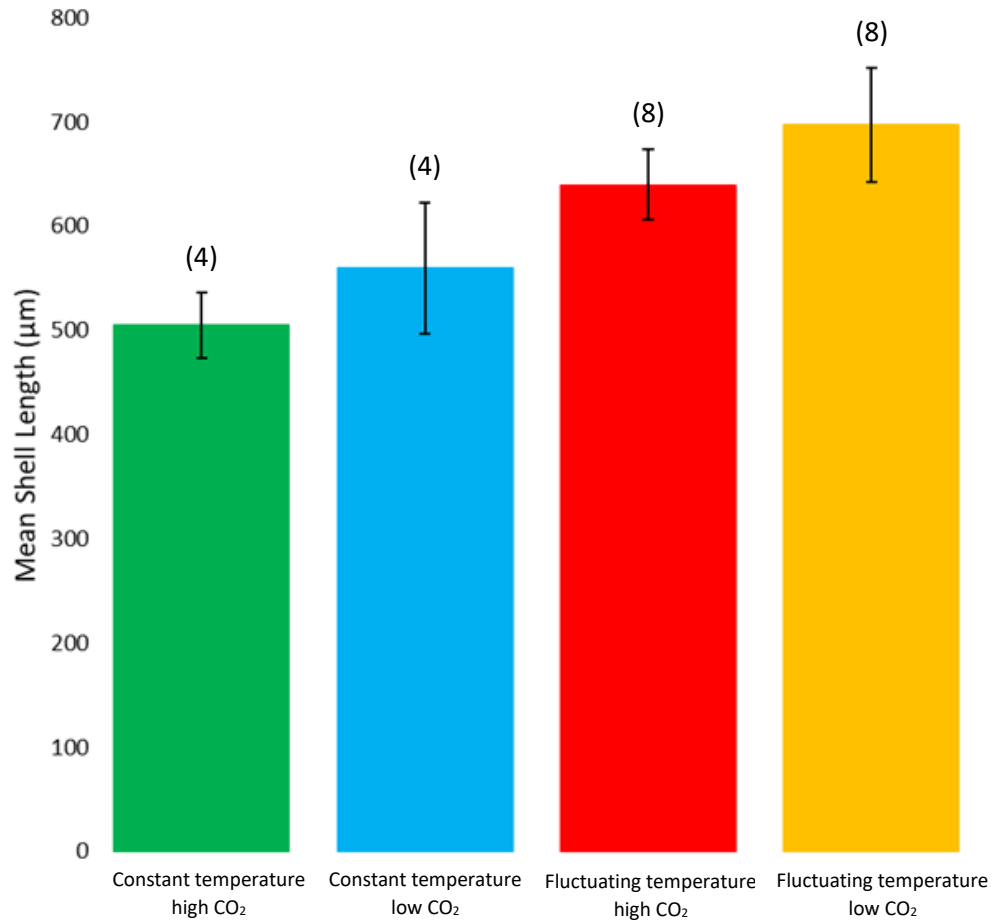


Figure 8. Mean shell length (µm) of post-set abalone in the four treatments. Columns represent mean. Error bars are ± standard deviation. Numbers in parentheses indicate sample size (n).

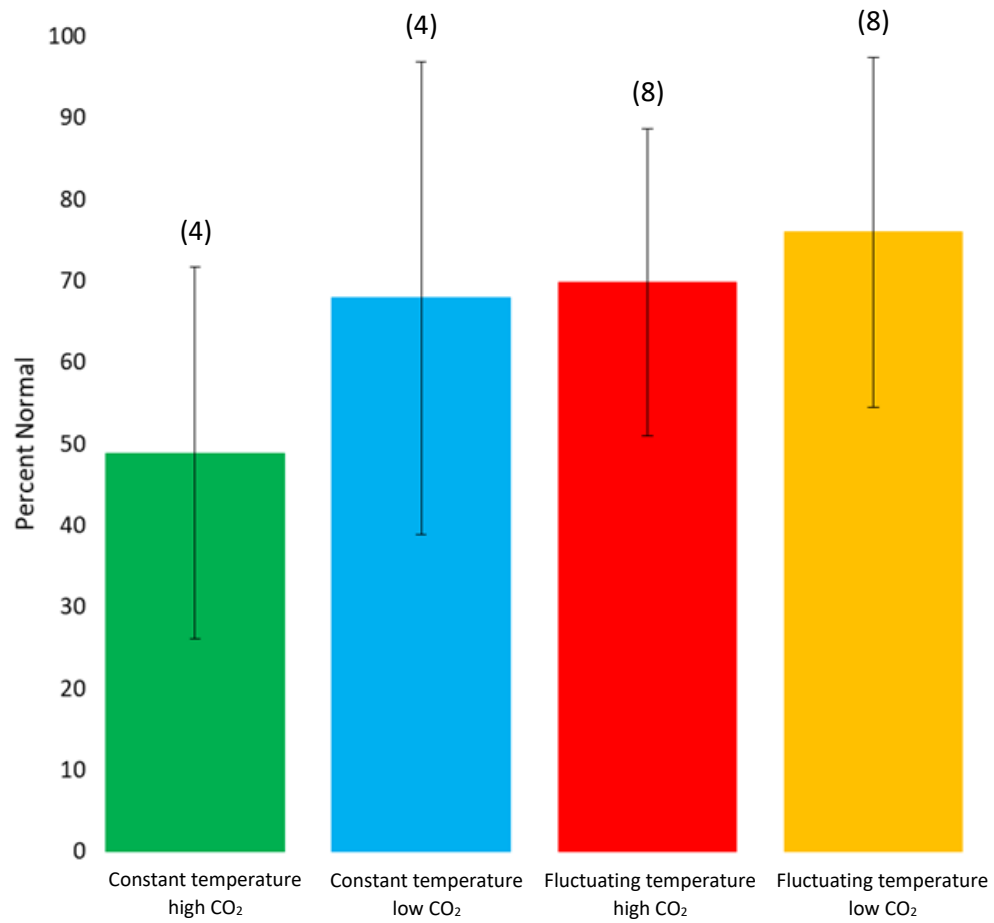


Figure 9. Percent normal shelled pinto abalone in the four treatments. Columns represent mean. Error bars are \pm standard deviation. Numbers in parentheses indicate sample size (n).

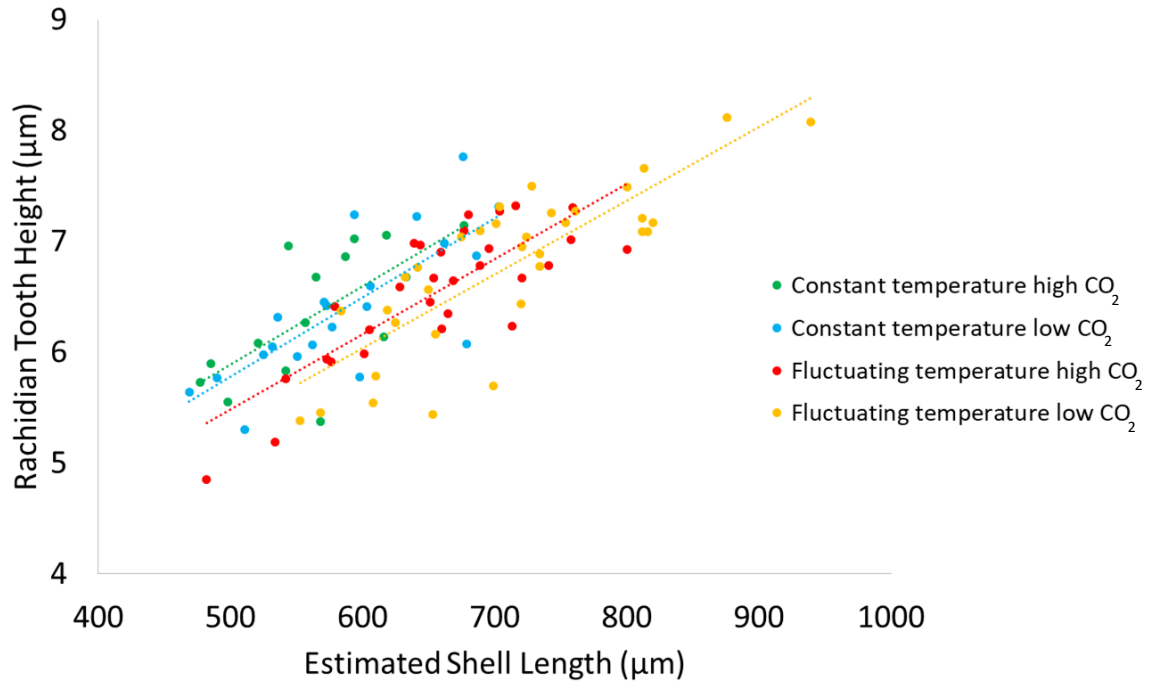


Figure 10. Rachidian tooth height (μm) as a function of estimated shell length (μm) for the four treatment groups. The red and yellow lines are below the blue and green lines, indicating rachidian tooth height is negatively affected by fluctuating temperature (Table 3).

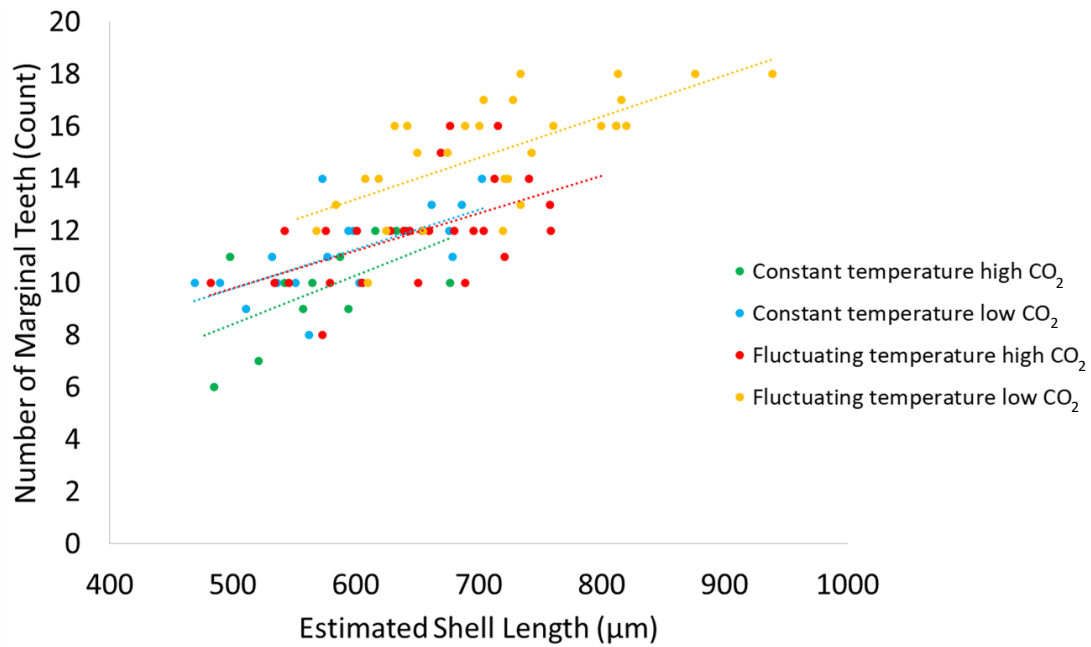


Figure 11. Number of marginal teeth (count) as a function of estimated shell length (μm) for the four treatment groups. Fluctuating temperature increased the number of marginal teeth, illustrated by the yellow line on top. High CO₂ decreased the number of marginal teeth, illustrated by the green line on bottom (Table 3).

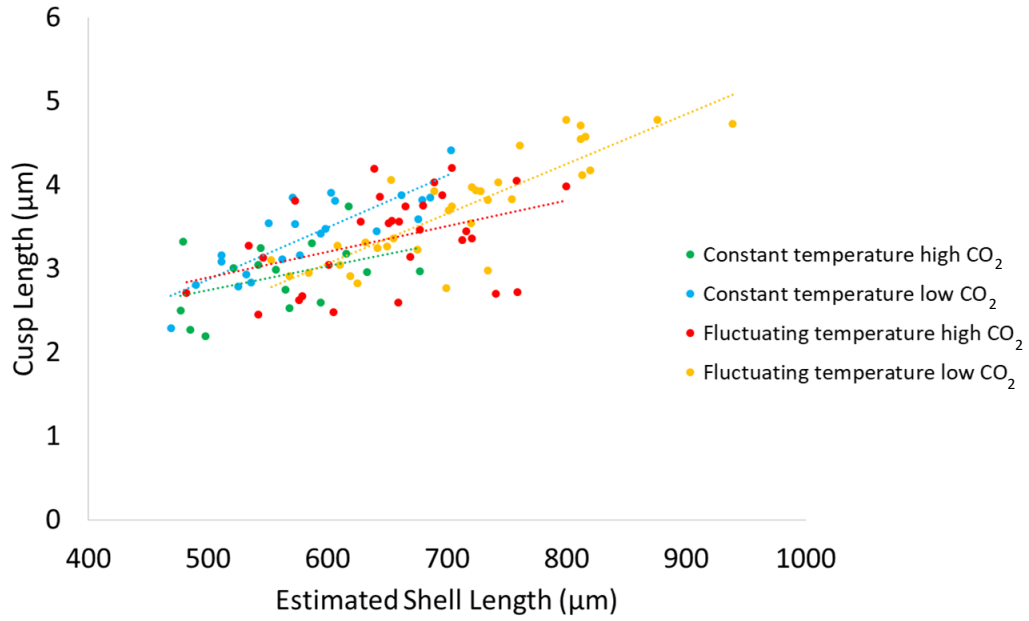


Figure 12. Cusp Length (μm) as a function of estimated shell length (μm) for the four treatment groups. The red and green lines are generally below the blue and yellow lines, indicating cusp length was negatively affected by high CO₂ (Table 3).

Table 3. Linear equations for trend lines in Figures 10, 11, and 12.

	Treatment:	Linear Equation:	R ² :
Rachidian tooth height as a function of estimated shell length (Figure 10)	Constant temperature low CO ₂	$y = 0.0072x + 2.19$	0.58
	Constant temperature high CO ₂	$y = 0.0071x + 2.35$	0.46
	Fluctuating temperature low CO ₂	$y = 0.0066x + 2.05$	0.68
	Fluctuating temperature high CO ₂	$y = 0.0068x + 2.10$	0.66
Number of marginal teeth as a function of estimated shell length (Figure 11)	Constant temperature low CO ₂	$y = 0.015x + 2.19$	0.40
	Constant temperature high CO ₂	$y = 0.019x - 0.96$	0.33
	Fluctuating temperature low CO ₂	$y = 0.016x + 3.75$	0.46
	Fluctuating temperature high CO ₂	$y = 0.014x + 2.61$	0.30
Cusp length as a function of estimated shell length (Figure 12)	Constant temperature low CO ₂	$y = 0.0062x - 0.23$	0.71
	Constant temperature high CO ₂	$y = 0.0029x + 1.30$	0.17
	Fluctuating temperature low CO ₂	$y = 0.0059x - 0.50$	0.72
	Fluctuating temperature high CO ₂	$y = 0.0031x + 1.35$	0.18

and number of marginal teeth (Figure 11), but high CO₂ did not affect as many parameters as fluctuating temperature did (Table 2). Neither of the treatments significantly affected the rachidian tooth base width, buccal cartilage position, or full length of the radula (Table 2).

Geometric Analysis

A principal components analysis (PCA) determined the major differences in radula orientation between the treatments (Figure 13). Principal component one explained 37.3% of the shape variance and captured the differences in vertical orientation (Figure 13, x-axis). Principal component two explained 16.9% of the shape variance and captured differences in the horizontal orientation of the teeth, most notably in the rachidian tooth being to the left or the right of average (Figure 13, y-axis).

The orientation of the middle five teeth was not significantly affected by either temperature regimen or CO₂, or the interaction between them (Procrustes ANOVA, $F= 0.83$, $p=0.52$, Table 4). To determine the relationship between the four treatment groups, I plotted the groups on a phylogenetic tree as if they were species groups (Figure 14). Treatment groups with similar regimens (for example, both high CO₂ groups) do not have similar principal component scores. This demonstrates that the treatments did not affect principal component scores, and thus did not affect the orientation of the middle five radula teeth (Figure 15).

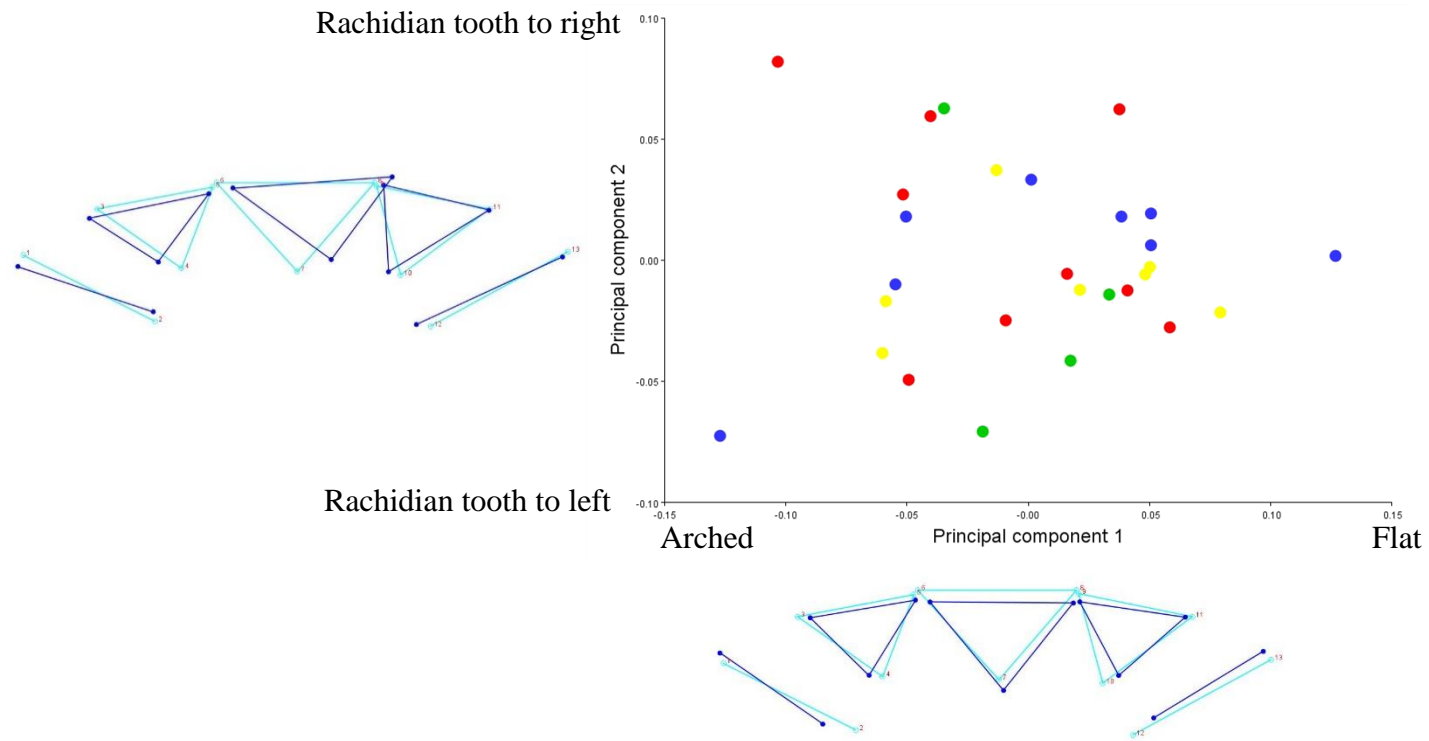


Figure 13. Results of a principal components analysis (PCA) for radula shape. Graph is a PCA score plot with points of PCA scores for each radula. Colors are consistent with Figure 1. On the x-axis, wireframe of principal component one (PC1). Light blue is the radula orientation for a PC1 of 0.0. Dark blue shows a high PC1 score, with the outer dark blue lines on the inside and the rachidian tooth positioned lower than the light blue lines, illustrating a row that is flat. On the y-axis, wireframe of principal component two (PC2). Light blue is the radula orientation for a PC2 of 0.0. Dark blue shows a high PC2 score, with the rachidian tooth to the right.

Table 4. Procrustes ANOVA output for geometric radula morphological analysis.

Procrustes ANOVA	<i>shape ~ Temperature + CO₂ + Temperature*CO₂</i>						
	Df	SS	MS	Rsq	F	Z	p value
Temperature	1	0.007	0.007	0.028	0.736	-0.321	0.621
CO ₂	1	0.005	0.005	0.022	0.580	-0.802	0.795
Temperature:CO ₂	1	0.008	0.008	0.032	0.835	-0.062	0.521
Residuals	24	0.226	0.009	0.918			
Total	27	0.246					

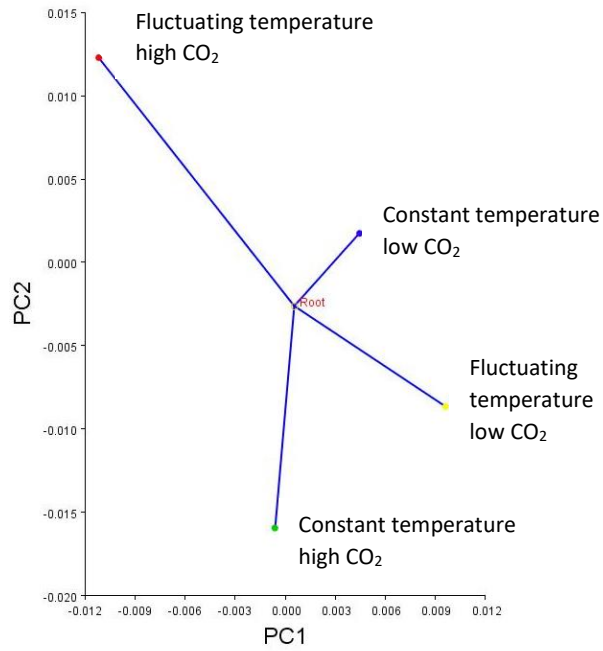


Figure 14. A phylogenetic tree illustrating the relatedness between the four treatment groups for principal component one (PC1) and principal component two (PC2). Similar treatment regimens do not have similar scores, indicating that the treatments did not affect radula orientation.

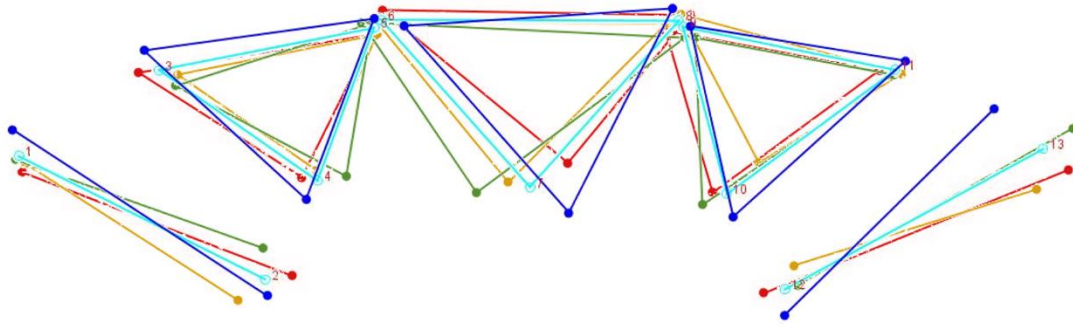


Figure 15. Overlapping wireframes demonstrate the differences in orientation of the middle five radula teeth for each treatment. Light blue is the average orientation for all of the treatments (PC1 and PC2 scores are 0.0). Other colors represent the average orientation of the treatment group as consistent with Figure 1. Constant temperature low CO₂ (dark blue) has a flat vertical orientation with the rachidian tooth to the right. Constant temperature high CO₂ treatment (green) has a vertical orientation near the middle, between flat and arched (PC1 score near 0.0) and the rachidian tooth is far to the left. Fluctuating temperature low CO₂ treatment (yellow) has a more flat vertical orientation and the rachidian tooth is slightly to the left. Fluctuating temperature high CO₂ treatment (red) has an arched vertical orientation with the rachidian tooth to the right.

DISCUSSION

I investigated the impact of fluctuating temperature and high CO₂ on the survival, growth, and shell and radula morphology of pinto abalone (*Haliotis kamtschatkana*) post-sets. I predicted that both fluctuating temperature and high CO₂ would negatively affect post-sets. I found that high CO₂ conditions were overall detrimental to pinto abalone, but fluctuating temperatures did not have consistently negative consequences.

Fluctuating Temperature

Survival was negatively affected by fluctuating temperature, as demonstrated by the fluctuating temperature low CO₂ treatment group having the lowest overall percent survival (12%). This finding is supported by observations at the PSRF hatchery where fluctuating temperatures in rearing tanks led to high mortality of pinto abalone larvae and post-sets (Caitlin O'Brien, personal communication).

Although survival decreased under fluctuating temperature, shell length appeared to be positively affected. The positive effect observed on growth is most likely associated with the higher temperatures that the fluctuating temperature regimen reached, compared to the constant temperature, not the fluctuation itself. For example, if the fluctuation had spanned 4°C in the opposite direction, going from 10°C down to 6°C and back again, the growth in this treatment likely would have been less than the constant 10°C treatment, due to individuals in this hypothetical treatment spending more time at lower temperatures. My findings are supported by Cummings et al. (2019) who also found greater growth at higher temperatures. Under 15°C, New Zealand pāua (*Haliotis iris*) juvenile shell length increased by 34% in four months, compared to

only a 22% increase in shell length under 13°C. Similarly, wild pinto abalone growth is observed to be greatest during the summer months when temperature at depth is higher (Neuman et al. 2018).

The appearing conflicting findings between survival and shell length could be explained by three mechanisms. First, within the preferred temperature range of pinto abalone, increases in temperature are associated with increases in growth (Morash and Alter, 2016). Higher temperature can also lower survival for smaller individuals (Searle et al. 2006) making it more likely for larger individuals to survive to be measured. However, temperature increases are also associated with increased respiration (Morash and Alter, 2016), which could decrease the amount of energy allocated to growth, negatively affecting growth. The balance between respiration and growth in post-set pinto abalone warrants further investigation.

Second, higher temperature makes precipitation of aragonite out of seawater more efficient (Kroeker et al. 2013), making the building blocks for shell formation easier to obtain. This was not observed in my experiment due to the fluctuating temperature treatments having lower average aragonite saturation than the corresponding constant temperature treatments. Aragonite was supersaturated in all of my treatment groups, though proper shell calcification could require even greater saturation states. For example, proper development of oyster larvae requires $\Omega_{\text{aragonite}} > 1.7$, especially during the first 48 hours post fertilization (Barton et al. 2015). Calcification was not directly measured in my study, so the mechanism behind the relationship between observed growth and aragonite saturation state is unclear.

Third, competition between individuals within the wells of the six-well plate could also potentially explain why only the largest post-set abalone survived. This mechanism is extremely unlikely due to observations of well-established diatom films in all the six-well plates. Diatom

films grew well in all the free-standing incubators, but took longer to become established in the walk-in incubator. I observed that six-well plates in the high CO₂ treatments, with potentially greater access to CO₂, often had diatom films that appeared darker and thicker. The difference in CO₂ between my treatment groups could have resulted in differences in the carbon to nitrogen ratio in the diatoms, affecting the nutritional content, but no data on diatoms was collected. In addition, Kuehl and Donovan (2020) did not see any competitive effects of keeping ten post-set abalone in each well of a six-well plate. However, the traditional radula morphology analysis indicated that the fluctuating temperature treatment resulted in more, smaller teeth formed closer together. Radula rows that are closer together facilitate eating small food items, such as diatoms (Kawamura et al. 2001). The individuals in the fluctuating temperature treatments were possibly better at eating diatoms than those in the constant temperature treatments, contributing to greater growth. This mechanism does not, however, also support the low survival demonstrated by this treatment.

Overall, my findings indicate that higher temperatures, the fluctuations of which could be made more severe by ocean warming, are detrimental to post-set pinto abalone survival, though those that survive may have larger shells that will aid in protection from predators.

Elevated CO₂

There was a large difference between expected and actual pCO₂ measured in this experiment, making interpretation of results difficult. The overgrowth of photosynthetic diatom food in the wells with the post-set abalone likely removed much of the CO₂ from the water. FSW from the carboys used in weekly water changes was likely closer to the desired 400 ppm or 1200

ppm treatment. When adding FSW, the $p\text{CO}_2$ in the six-well plate probably increased. Then the CO_2 was utilized by diatoms throughout the week which lowered the $p\text{CO}_2$ until the next week's water change when $p\text{CO}_2$ increased again. Water samples were only collected at the end of the week, right before the water change, at which point the $p\text{CO}_2$ was probably at its lowest. In this way, the $p\text{CO}_2$ was also fluctuating in this experiment, not being held at two different constant amounts. There appeared to be greater growth of diatoms in the high CO_2 treatment groups, which could have contributed to the greater difference between expected and actual $p\text{CO}_2$ measurements in the high CO_2 treatments over the low CO_2 treatments, although the growth of diatoms was not measured. In addition, water chemistry analysis was not conducted on water from the carboys used in weekly water changes. It is unknown if this water was actually in equilibrium with the CO_2 mixture bubbled into it, likely further contributing to the difference between expected and observed $p\text{CO}_2$.

Post-set pinto abalone treated with high CO_2 were negatively affected such that shell length was 5% smaller under high CO_2 compared to low CO_2 . These findings are consistent with Crim et al. (2011) who also found a 5% decrease in shell size for their 800 ppm CO_2 treatment, compared to their 400 ppm CO_2 treatment. This finding supports high CO_2 related ocean acidification negatively impacting calcification of the shell, although calcification was not directly measured in my study. The aragonite saturation state was greater than one throughout my experiment, indicating that the building blocks for successful calcification should have been available. However, successful calcification might require an even greater saturation state. In addition, lower pH created by elevated CO_2 makes other processes like respiration more stressful, leading to less energy going towards growth (Morash and Alter, 2016). Whether

through decreasing calcification, influencing the allocation of energy resources, or both, elevated CO₂ had a negative impact on shell length.

An initially surprising finding to me, given the significant difference in shell length, was the similarity in percent survival between the high and low CO₂ treatments under constant temperature. Consistent with this finding, European abalone (*Haliotis tuberculata*) juveniles exposed for three months to lower pH (7.6) exhibited significantly smaller shell length (grew only 1.8 mm) compared to ambient pH (7.8, grew 2.7 mm), but had no significant difference in percent survival (ranging between $90.9 \pm 10.3\%$ and $96 \pm 3.3\%$) (Auzoux-Bordenave et al. 2020). The negative effects of high CO₂ on shell length did not lead directly to lower survival. However, under natural environmental conditions, a post-set abalone with a smaller sized shell could be less fit for survival from predation.

Though differences in shell morphology between high and low CO₂ would be anticipated, they were not observed in this study. This could be due to the unexpected fluctuations in pCO₂ modifying my planned treatment regimens. My findings are in contrast to Crim et al. (2011) who did find significant differences in the percent normal shelled larval pinto abalone between CO₂ treatments. Under 400 ppm CO₂, 2% of pinto abalone larvae developed abnormal shells, while under 800 ppm CO₂, 40% of larva developed abnormal shells and under 1800 ppm CO₂, 99% of larva developed abnormal shells (Crim et al. 2011). Similarly, Auzoux-Bordenave et al. (2020) found that shell mineralization of European abalone (*H. tuberculata*) juveniles was negatively affected by low pH such that their shells formed irregular edges and had several small holes as a result of corrosion. Both these sources of evidence suggest that abalone larvae and abalone juveniles exhibit abnormal shell morphologies when developing under low pH conditions. Thus, the post-set life stage, which lies between the larvae and juvenile life stages, is assumed to

exhibit abnormalities in shell morphology as well. In the constant temperature high CO₂ treatment in my experiment, I observed that 43% of post-set pinto abalone had abnormal shells, consistent with the above evidence. However, this finding was not significant due to the other high CO₂ treatment group, with fluctuating temperature, performing similarly to both low CO₂ treatment groups, with only 27% of post-set pinto abalone exhibiting abnormal shells. This demonstrates that fluctuating temperature can possibly mitigate the negative effects of elevated CO₂ on the shell. This is possible due to, as discussed earlier, higher temperatures increasing precipitation of aragonite out of solution, making shell formation easier.

Interaction between temperature and CO₂

An overall surprising finding in this study were the results of the fluctuating temperature high CO₂ treatment group. I hypothesized that this treatment group would perform the worst but it did not. Fluctuating temperature and high CO₂ had the second highest percent survival (32.6%), second greatest mean shell length ($641 \pm 91 \mu\text{m}$), and the second highest mean proportion of normal shelled individuals (70%). When comparing this treatment group with the constant temperature high CO₂ treatment, there is similar survival (~32%), but the fluctuating temperature yields a greater mean shell length (a difference of 133 μm) and greater percent normal shelled individuals. This is evidence of fluctuating temperature mitigating the negative effects of high CO₂ on the shell. This is likely due to higher temperatures either increasing aragonite precipitation or increasing the metabolic rate of the post-set abalone, both of which can increase shell building and repair. These findings are supported by a recent study on European abalone (*H. tuberculata*) larvae which also found a higher proportion of normal shelled

individuals at higher temperatures under low pH conditions (Kavousi et al. 2022). European abalone larvae reared to 72 hours post-fertilization in a pH of 7.7 resulted in 58% of larvae fully shelled at 17°C and a higher, 62% of larvae fully shelled at 19°C (Kavousi et al. 2022, Supplementary Data). The higher temperature mitigated the negative effects of high CO₂, allowing shells to fully develop even in low pH conditions. The mitigation observed in my experiment indicates that pinto abalone post-sets could be successfully outplanted under predicted ocean warming and acidification conditions as both the temperature and amount of dissolved CO₂ in the Salish Sea are predicted to rise in concert. Further research is paramount to determine the extent of the mitigating effects and if these effects are observed in this life stage only or can be applied across all life stages.

Radula

The traditional radula analysis showed that five descriptive radula parameters were affected, either positively (total number of rows and the number of marginal teeth) or negatively (rachidian tooth height, gap length, and radula width) by the fluctuating temperature treatment, leading to a more compact radula with a greater number of rows formed closer together. This could be explained by the fluctuating temperature altering energy allocation between respiration and radula growth, though an energy budget for post-set pinto abalone was not calculated. These findings are in contrast to Sigwart and Carey (2014) who found no difference in the number of radula rows between chitons (*Leptochiton asellus*) exposed to 10°C, 15°C, or 20°C. The authors concluded that the increase in metabolic activity and therefore feeding associated with increased temperatures was mitigated by an increase in radula growth (Sigwart and Carey, 2014), such that

the overall number of rows was not increasing, but the replacement of new teeth was. Feeding rate, respiration, and wear or breakage of teeth was not measured in my experiment. Thus, additional experimentation is necessary to determine mechanisms behind my observations. My findings indicate that ocean warming could affect radula development, causing pinto abalone to develop more compact radulae.

High CO₂ negatively affected only two parameters (cusp length and number of marginal teeth). These effects indicate that high CO₂ is creating smaller teeth which could be occurring through removing building blocks required for biomineralization from the water, or by causing other stress to the abalone, resulting in lower energetic resources available to put towards radula growth or repair. These findings are consistent with Marchant et al. (2010) who found lower radula area in common limpets (*Patella vulgata*) exposed to low pH for five days. Common limpets lost ~1700 nm² of radula tooth area under low pH (7.6) compared to ~500 nm² of radula tooth area under normal pH (8.2) (Marchant et al. 2010). My findings indicate that ocean acidification could affect radula development, causing pinto abalone to develop slightly smaller radula teeth.

The geometric analysis did not find any difference in the orientation of the radula teeth between treatment groups, indicating that the overall shape of the radula was not affected by ocean warming or acidification.

Abalone radula morphology changes as they grow and transition into new life stages (Kawamura et al. 2001, Kuehl and Donovan, 2020, Onitsuka et al. 2004). The post-set stage begins right after metamorphosis and lasts for around three months (90 days). My organisms were 40 days post-settlement at the time of preservation. The transition from post-set to juvenile is marked by a transition in diet from diatoms to macroalgae that is facilitated by a change in

radula morphology. Radula rows that are closer together are characteristic of post-sets because this shape makes eating small food items, such as diatoms, easier (Kawamura et al. 2001). Radula rows that are further apart are characteristic of juveniles due to this shape being better for eating larger food, like macroalgae (Kawamura et al. 2001). The fluctuating temperature treatment resulted in post-set radulae that are more compact than those from the constant temperature. The influence that this modification could have on the eventual transition to eating macroalgae during the juvenile stage is unknown and important to understand for future survival. Juveniles with compact radulae could possibly have lower survival because they cannot as efficiently eat macroalgae. A long term experiment that exposes pinto abalone from settlement, throughout the whole post-set stage, and into the juvenile stage to fluctuating temperatures is justified.

My findings are the first to quantify impacts on the pinto abalone radula, or any abalone radula, due to water chemistry. Together, my findings indicate that surviving pinto abalone post-sets will have more compact radula and smaller radula teeth under future ocean warming and acidification conditions. The ability of pinto abalone post-sets to eat, survive, and eventually fulfill their ecological niche when they transition into later life stages with a compact radula morphology is unknown and warrants further investigation.

Conclusion

Pinto abalone recovery efforts by the Puget Sound Restoration Fund (PSRF) and other groups in the Salish Sea would be best served by using outplant locations where temperatures are near constant (around 10°C) and CO₂ is low (pH is near 8.2). This type of location has the

potential to yield the greatest survival and the best chance of normal shell and radula development, promoting population recovery. This conclusion is based on evidence presented in this thesis which found that a single stressor is detrimental to post-set pinto abalone: fluctuating temperature alone decreased survival and high CO₂ alone decreased shell length, which would make individuals in the wild more vulnerable to predation.

In the field, constant water chemistry conditions are very rare due to seasonality, tides, currents, and other location dependent influences (Lowe et al. 2019). Range and frequency of fluctuations in water chemistry parameters are variable at different locations, creating outplant sites with smaller or greater fluctuations in temperature and/or pH. Carson et al. (2019) found that outplant sites varied in survivorship and concluded that survival of outplanted individuals was due to site specific factors. Temperature data at the outplant sites was collected with loggers which recorded temperature every 15 minutes for almost five years, yet specifics on fluctuations of temperature at the outplant sites were not reported (Carson et al. 2019). Re-evaluating the temperature data collected could help explain the differences in survivorship. Sites with low survival could be those with greater range and frequency of temperature fluctuations. For example, my data indicate that outplant sites with larger temperature fluctuations, increasing then decreasing by 4°C each week, will have lower survival than sites with smaller temperature fluctuations that stay closer to an average of 10°C. This would make outplanting at sites with smaller fluctuations in temperature more effective for restoration.

Similarly, CO₂, and thus pH, are also variable throughout the year, mostly due to net ecosystem respiration (Lowe et al. 2019). Data on pH at the outplant sites is lacking. However, complete water chemistry data including temperature, pH, dissolved oxygen, salinity, and more is currently being collected (Eileen Bates, personal communication). When data on pH is

collected and finalized, it can be used by PSRF to evaluate outplant sites. Outplant sites that are characterized by lower $p\text{CO}_2$ and corresponding higher pH, near 8.2, are expected to have greater growth than locations with slightly higher $p\text{CO}_2$ and slightly lower pH, near 8.0, making those outplant locations more effective for the recovery of pinto abalone. My study is appropriately timed for PSRF to use my findings along with the new water chemistry data to evaluate the outplant sites and re-select which sites to use for future outplanting.

In addition to outplant site evaluation, outplant methodology evaluation can utilize this study as well. Currently PSRF outplants juveniles that are one to two years in age which requires a large investment of resources. Shifting outplanting to earlier life stages could lower the cost per individual. Mills-Orcutt et al. (2020) outplanted larvae given a settlement cue into tented and open larval abalone modules. Survival in the field after four months was 0.4% in tented modules (Mills-Orcutt et al. 2020). Water chemistry conditions at the locations where the tented modules were placed were not collected. Survival could potentially be higher if these conditions were known and used to place the modules in more favorable locations.

Future ocean warming and acidification have the ability to modify current variations in temperature and CO_2 (pH) in the Salish Sea (Lowe et al. 2019) and thus at the outplant sites. This makes the consistent collection of water chemistry data and re-evaluation of outplant sites over time important. My findings indicate that the combination of stressors, fluctuating temperature and high CO_2 together, exhibited similar survival and increased shell length compared to the absence of stressors. Outplant sites that show simultaneous increases in temperature and decreases in pH should still be able to sustain pinto abalone survival and proper development. As ocean warming and acidification continue to rise in concert, pinto abalone post-sets can be successfully outplanted into the Salish Sea.

LITERATURE CITED

- Adams, D.C., and E. Otarola-Castillo. 2013. Geomorph: an R package for the collection and analysis of geometric morphometric shape data. *Methods in Ecology and Evolution* 4:393-399.
- Auzoux-Bordenave, S., N. Wessel, A. Badou, S. Martin, S. M'Zoudi, S. Avignon, S. Roussel, S. Huchette, and P. Dubois. 2020. Ocean acidification impacts growth and shell mineralization in juvenile abalone (*Haliotis tuberculata*). *Marine Biology* 167(1):1–14.
- Avignon, S., S. Auzoux-Bordenave, S. Martin, P. Dubois, A. Badou, M. Coheleach, N. Richard, S. Di Giglio, L. Malet, A. Servili, F. Gaillard, S. Huchette, and S. Roussel. 2020. An integrated investigation of the effects of ocean acidification on adult abalone (*Haliotis tuberculata*). *ICES Journal of Marine Science* 77(2):757–772.
- Babcock, R., and J. Keesing. 1999. Fertilization biology of the abalone *Haliotis laevigata*: Laboratory and field studies. *Canadian Journal of Fisheries and Aquatic Sciences* 56(9):1668–1678.
- Barton, A., G.G. Waldbusser, R.A. Feely, S.B. Weisberg, J.A. Newton, B. Hales, S. Cudd, B. Eudeline, C.J. Langdon, I. Jefferds, T. King, A. Suhrbier, and K. McLaughlin. 2015. Impacts of coastal acidification on the Pacific Northwest shellfish industry and adaptation strategies implemented in response. *Oceanography* 28(2):146–159.
- Boulais, M., K.J. Chenevert, A.T. Demey, E.S. Darrow, M.R. Robison, J.P. Roberts, and A. Volety. 2017. Oyster reproduction is compromised by acidification experienced seasonally in coastal regions. *Scientific Reports* 7(1): 1–9.
- Bouma, J.V., D.P. Rothaus, K.M. Straus, B. Vadopalas, and C.S. Friedman. 2012. Low juvenile pinto abalone *Haliotis kamtschatkana kamtschatkana* abundance in the San Juan Archipelago, Washington State. *Transactions of the American Fisheries Society* 141(1):76–83.
- Byrne, M., M. Ho, E. Wong, N.A. Soars, P. Selvakumaraswamy, H. Shepard-Brennand, S.A. Dworjanyn, and A.R. Davis. 2011. Unshelled abalone and corrupted urchins: Development of marine calcifiers in a Changing Ocean. *Proceedings of the Royal Society B: Biological Sciences* 278(1716): 2376–2383.
- Calderón-Liévanos, S., N.Y. Hernández-Saavedra, S.E. Lluch-Cota, P. Cruz-Hernández, F.D.J. Ascencio-Valle, and M.T. Sicard. 2019. Survival and respiration of green abalone (*Haliotis fulgens*) facing very short-term marine environmental extremes. *Marine and Freshwater Behaviour and Physiology* 52:1: 1-15.
- Carson, H.S., D.J. Morin, J.V. Bouma, M. Ulrich, and R. Sizemore. 2019. The survival of hatchery-origin pinto abalone *Haliotis kamtschatkana* released into Washington waters. *Aquatic Conservation: Marine and Freshwater Ecosystems* 29(3):424–441.

- Carson, H.S. and M. Ulrich. 2019. Status report for the pinto abalone in Washington. Washington Department of Fish and Wildlife, Olympia, Washington. iii + 25 pp.
- Crim, R.N., J.M. Sunday, and C.D.G. Harley. 2011. Elevated seawater CO₂ concentrations impair larval development and reduce larval survival in endangered northern abalone (*Haliotis kamtschatkana*). *Journal of Experimental Marine Biology and Ecology* 400(1–2):272–277.
- Cummings, V.J., A.M. Smith, P.M. Marriott, B.A. Peebles, and N.J. Halliday. 2019. Effect of reduced pH on physiology and shell integrity of juvenile *Haliotis iris* (pāua) from New Zealand. *PeerJ* 2019(9):1–23.
- Donovan, D.A., and T.H. Carefoot. 1998. Effect of activity on energy allocation in the northern abalone, *Haliotis kamtschatkana* (Jonas). *Journal of Shellfish Research* 17(3):729-736.
- Emanuel, M.P., D. Pillay, M. van der Merwe, and G.M. Branch. 2020. Interactive effects of pH and temperature on native and alien mussels from the west coast of South Africa. *African Journal of Marine Science* 42(1):1-12.
- Evans, W., K. Pocock, A. Hare, C. Weekes, B. Hales, J. Jackson, H. Gurney-Smith, J.T. Mathis, S.R. Alin, and R.A. Feely. 2019. Marine CO₂ patterns in the Northern Salish Sea. *Frontiers in Marine Science* 5:1–18.
- Gaume, B., M. Fouchereau-Peron, A. Badou, M-N. Helléouet, S. Huchette, and S. Auzoux-Bordenave. 2011. Biomineralization markers during early shell formation in the European abalone *Haliotis tuberculata*, Linnaeus. *Marine Biology* 158:341–353.
- Horwitz, R., T. Norin, S.A. Watson, J.C.A. Pistevos, R. Beldade, S. Hacquart, J.P. Gattuso, R. Rodolfo-Metalpa, J. Vidal-Dupirol, S.S. Killen, and S.C. Mills. 2020. Near-future ocean warming and acidification alter foraging behaviour, locomotion, and metabolic rate in a keystone marine mollusc. *Scientific Reports* 10(1):1–12.
- IPCC. 2014. Summary for policymakers. In: *Climate Change 2014: Impacts, Adaptation, and Vulnerability. Part A: Global and Sectoral Aspects. Contribution of Working Group II to the Fifth Assessment Report of the Intergovernmental Panel on Climate Change* [Field, C.B., V.R. Barros, D.J. Dokken, K.J. Mach, M.D. Mastrandrea, T.E. Bilir, M. Chatterjee, K.L. Ebi, Y.O. Estrada, R.C. Genova, B. Girma, E.S. Kissel, A.N. Levy, S. MacCracken, P.R. Mastrandrea, and L.L. White (eds.)]. Cambridge University Press, Cambridge, United Kingdom and New York, New York, USA, pp. 1-32
- Kavousi, J., S. Roussel, S. Martin, F. Gaillard, A. Badou, C. Di Poi, S. Huchette, P. Dubois, and S. Auzoux-Bordenave. 2022. Combined effects of ocean warming and acidification on the larval stages of the European abalone *Haliotis tuberculata*. *Marine Pollution Bulletin* 113131.

- Kawamura, T., H. Takami, R.D. Roberts, and Y. Yamashita. 2001. Radula development in abalone *Haliotis discus hannai* from larva to adult in relation to feeding transitions. *Fisheries Science* 67:596–605.
- Keppel, E.A., R.A. Scrosati, and S.C. Courtenay. 2015. Interactive effects of ocean acidification and warming on subtidal mussels and sea stars from Atlantic Canada. *Marine Biology Research* 11(4):337–348.
- Klingenberg, C.P. 2011. MorphoJ: An integrated software package for geometric morphometrics. *Molecular Ecology Resources* 11:353-357.
- Kroeker, K.J., R.L. Kordas, R.N. Crim, and G.G. Singh. 2010. Meta-analysis reveals negative yet variable effects of ocean acidification on marine organisms. *Ecology Letters* 13(11):1419–1434.
- Kroeker, K.J., R.L. Kordas, R. Crim, I.E. Hendriks, L. Ramajo, G.S. Singh, C.M. Duarte, and J-P. Gattuso. 2013. Impact of ocean acidification on marine organisms: Quantifying sensitivities and interaction with warming. *Global Change Biology* 19:1884-1896.
- Kroeker, K.J., E. Sanford, B.M. Jellison, and B. Gaylord. 2014. Predicting the effects of ocean acidification on predator-prey interactions: A conceptual framework based on coastal molluscs. *Biological Bulletin* 226(3):211–222.
- Kuehl, L.M., and D.A. Donovan. 2020. Survival, growth, and radula morphology of *Haliotis kamtschatkana* postlarvae fed six species of benthic diatoms. *Aquaculture* 736136.
- Lawlor, J.A., and S.M. Arellano. 2020. Temperature and salinity, not acidification, predict near-future larval growth and larval habitat suitability of *Olympia* oysters in the Salish Sea. *Scientific Reports* 10(1):1–15.
- Li, J., Z. Jiang, J. Zhang, J.W. Qiu, M. Du, D. Bian, and J. Fang. 2013. Detrimental effects of reduced seawater pH on the early development of the Pacific abalone. *Marine Pollution Bulletin* 74(1):320–324.
- Love, B.A., M.B. Olson, and T. Wuori. 2017. Technical note: a minimally invasive experimental system for pCO₂ manipulation in plankton cultures using passive gas exchange (atmospheric carbon control simulator). *Biogeosciences* 14:2675–2684.
- Lowe, A.T., J. Bos, and J. Ruesink. 2019. Ecosystem metabolism drives pH variability and modulates long-term ocean acidification in the Northeast Pacific coastal ocean. *Scientific Reports* 9(1):1–11.
- Marchant, H.K., P. Calosi, and J.I. Spicer. 2010. Short-term exposure to hypercapnia does not compromise feeding, acid-base balance or respiration of *Patella vulgata* but surprisingly is accompanied by radula damage. *Journal of the Marine Biological Association of the United Kingdom* 90(7):1379-1384.

- Mills-Orcutt, K.A., J.V. Bouma, and D.A. Donovan. 2020. Outplanting larval pinto abalone *Haliotis kamtschatkana kamtschatkana* (Jonas) as a recovery tool in the Salish Sea. *Journal of Shellfish Research* 39(2):381-88.
- Morash, A.J. and K. Alter. 2016. Effects of environmental and farm stress on abalone physiology: Perspectives for abalone aquaculture in the face of global climate change. *Reviews in Aquaculture* 8:342–368.
- Neuman, M. J., S. Wang, S. Busch, C. Friedman, K. Gruenthal, R. Gustafson, D. Kushner, K. Stierhoff, G. Vanblaricom, and S. Wright. 2018. A status review of Pinto Abalone (*Haliotis kamtschatkana*) along the west coast of North America: Interpreting trends, addressing uncertainty, and assessing risk for a wide-ranging marine invertebrate. *Journal of Shellfish Research* 37(4):869–910.
- Olsen, A.M. and M.W. Westneat. 2015. StereoMorph: an R package for the collection of 3D landmarks and curves using a stereo camera set-up. *Methods in Ecology and Evolution* 6:351-356.
- Onitsuka, T., T. Kawamura, S. Ohashi, T. Horii, and Y. Watanabe. 2004. Morphological changes in the radula of abalone *Haliotis diversicolor aquatilis* from post-larva to adult. *Journal of Shellfish Research* 23:1079–1085.
- Orr, J.C., V.J. Fabry, O. Aumont, L. Bopp, S.C. Doney, R.A. Feely, A. Gnanadesikan, N. Gruber, A. Ishida, F. Joos, R.M. Key, K. Lindsay, E. Maier-Reimer, R. Matear, P. Monfray, A. Mouchet, R.G. Najjar, G-K. Plattner, K.B. Rodgers, C.L. Sabine, J.L. Sarmiento, R. Schlitzer, R.D. Slater, I.J. Totterdell, M-F. Weirig, Y. Yamanaka, and A. Yool. 2005. Anthropogenic ocean acidification over the twenty-first century and its impact on calcifying organisms. *Nature* 437:681-686.
- Pelletier, G., E. Lewis, and D. Wallace. 2012. co2.sys2.1.xls, a Calculator for the CO₂ System in Seawater for Microsoft Excel/VBA, Washington State Department of Ecology, Olympia, WA, Brookhaven National Laboratory, Upton, NY.
- Rasband, W.S. 1997. ImageJ. National Institutes of Health, Bethesda, Maryland, USA.
- Petraitis, P.S., and S.R. Dudgeon. 2020. Declines over the last two decades of five intertidal invertebrate species in the western North Atlantic. *Communications Biology* 3(1):1–7.
- Rogers-Bennett, L., B.L. Allen, and D.P. Rothaus. 2011. Status and habitat associations of the threatened northern abalone: Importance of kelp and coralline algae. *Aquatic Conservation: Marine and Freshwater Ecosystems* 21(6):573–581.
- Rothaus, D.P., B. Vadopalas, and C.S. Friedman. 2008. Precipitous declines in pinto abalone (*Haliotis kamtschatkana kamtschatkana*) abundance in the San Juan Archipelago, Washington, USA, despite statewide fishery closure. *Canadian Journal of Fisheries and Aquatic Sciences* 65(12):2703–2711.

- Searle, T., R.D. Roberts, and P.M. Lokman. 2006. Effects of temperature on growth of juvenile blackfoot abalone, *Haliotis iris* Gmelin. *Aquaculture Research* 37:1441-1449.
- Sigwart, J.D., and N. Carey. 2014. Grazing under experimental hypercapnia and elevated temperature does not affect the radula of a chiton (Mollusca, Polyplacophora, Lepidopleurida). *Marine Environmental Research* 102:73-77.
- Swezey, D.S., S.E. Boles, K.M. Aquilino, H.K. Stott, D. Bush, A. Whitehead, L. Rogers-Bennett, T.M. Hill, and E. Sanford. 2020. Evolved differences in energy metabolism and growth dictate the impacts of ocean acidification on abalone aquaculture. *Proceedings of the National Academy of Sciences of the United States of America* 117(42):26513–26519.
- Wessel, N., S. Martin, A. Badou, P. Dubois, S. Huchette, V. Julia, F. Nunes, E. Harney, C. Paillard, and S. Auzoux-Bordenave. 2018. Effect of CO₂-induced ocean acidification on the early development and shell mineralization of the European abalone (*Haliotis tuberculata*). *Journal of Experimental Marine Biology and Ecology* 508:52–63.
- Zippay, M.L., and G.E. Hofmann. 2010. Effect of pH on gene expression and thermal tolerance of early life history stages of red abalone (*Haliotis rufescens*). *Journal of Shellfish Research* 29(2):429–439.
- Zuur, A.F., E.N. Ieno, N.J. Walker, A.A. Saveliev, and G.M. Smith. 2009. *Mixed effects models and extensions in ecology with R*. Springer, New York, New York, USA.